IEEE Access
Multidisciplinary ⋮ Rapid Review ⋮ Open Access Journal

Received 9 January 2024, accepted 24 February 2024, date of publication 26 February 2024, date of current version 21 March 2024.

Digital Object Identifier 10.1109/ACCESS.2024.3370839

RESEARCH ARTICLE

A Harmony Search Switching Matrix Algorithm for Enhanced Performance of Solar PV Arrays During Non-Uniform Irradiance Scenarios

PRADYUMNA MALLICK[1], RENU SHARMA[1], (Senior Member, IEEE), PRIYA RANJAN SATPATHY[2], SUDHAKAR BABU THANIKANTI[2], (Senior Member, IEEE), AND NNAMDI I. NWULU[3], (Senior Member, IEEE)

[1]Department of Electrical Engineering, ITER, Siksha 'O' Anusandhan Deemed to be University, Bhubaneswar 751030, India
[2]Department of Electrical and Electronics Engineering, Chaitanya Bharathi Institute of Technology, Hyderabad 500075, India
[3]Centre for Cyber-Physical Food, Energy and Water Systems, University of Johannesburg, Johannesburg 2006, South Africa

Corresponding author: Sudhakar Babu Thanikanti (sudhakarbabu66@gmail.com)

ABSTRACT The power loss in the arrays due to non-uniform irradiances in the site is the most common scenario observed in a PV system. The irradiance non-uniformity occurs due to obstacles between actual irradiance and modules caused by dust and shadow of clouds, trees, and buildings in some portions of the array. This results in complications like mismatch, power reduction, deformed characteristics curves, failure of power tracking algorithms, and sometimes physical damage to the PV modules. Numerous solutions are present for mitigating the above complications among which the array reconfiguration gained a huge audience for ease of implementation, lower cost, and higher reliability but, each technique exhibits certain drawbacks. In this paper, a harmony search reconfiguration (HSR) algorithm for dynamic reconfiguration is proposed that has advantages in terms of simplicity, adaptability, convergence speed, reduced switch count, and arbitrary array application. The modeling and validation are done in the MATLAB platform using 5×5, 9×9, 9×5, and 3×3 arrays under various shading cases and compared with the 22 existing conventional, static, and dynamic techniques. The depth investigation shows the higher performance of the HSR with 24.64% and 12.28% higher performance than conventional and static techniques with lowest actual power deviation of -1.10% and equivalent performance to that of existing techniques with reduced complexities.

INDEX TERMS Hotspot, mismatch, partial shading, photovoltaic, power generation, reconfiguration.

I. INTRODUCTION

Partial shading in photovoltaic (PV) arrays is a pressing issue with multifaceted causes, effects, and impacts on system performance [1]. The causes of partial shading are diverse, ranging from natural sources like clouds, trees, and buildings, to soiling and the degradation of individual solar panels within an array [2]. These factors can lead to non-uniform irradiance distribution across the array, resulting in adverse effects such as mismatch losses, reduced energy production, and thermal imbalances [3]. Moreover, partial shading exacerbates the risk of hotspots and can induce reverse-bias conditions in shaded modules, increasing the chances of permanent damage [4]. Beyond its immediate effects, partial shading has a cascading impact on the entire PV system, diminishing its overall energy yield, harming the reliability of the entire array and forming multiple peaks in the power curves that confuse traditional maximum power point tracking (MPPT) algorithms, causing them to make incorrect decisions in selecting the optimal operating point [5]. So, addressing these challenges is crucial for improving the efficiency, longevity, and economic viability of PV systems.

Hybrid MPPT techniques have emerged as a powerful solution for enhancing global peak tracking in photovoltaic systems under partial shading [6]. These techniques use various optimization algorithm to decide the actual or global

The associate editor coordinating the review of this manuscript and approving it for publication was Zhehan Yi.

peak in the power curves and avoids false tracking of local peaks ensuring higher power output from the system [7]. Also, these techniques intelligently switch between different MPPT modes on real-time shading conditions, enabling the system to adapt swiftly to varying levels of irradiance across the array. Recently, a swarm intelligence-based MPPT has been proposed, compared with other methods, and resulted in a standard deviation, mean absolute error, successful rate, and efficiency of 3.95, 0.13, 98.88, and 99.89% respectively [8]. Similarly, a salp-swarm MPPT algorithm has been proposed in [9] resulting in unparalleled global exploration and local search capabilities, yielding heightened energy of 43.75%. Another Dandelion Optimizer MPPT technique has been proposed that achieved the highest average efficiency at 99.60% surpassing other techniques [10]. Some other techniques include SA-P&O [11], voltage scanning method [12], marine predator [13], modified honey badger [14] algorithms, etc. that deal with the issue of the local peak convergence and ensure global peak tracking from the distorted power curves. However, increased complexity in hardware and software, higher implementation and control costs, algorithm selection and tuning, and reliability during realistic partial shading scenarios are the major drawbacks encountered by these techniques in real-time systems.

PV array reconfiguration emerges as a promising solution that can mitigate some of the drawbacks associated with the implementation of hybrid MPPT techniques in PV systems [15]. Array reconfiguration offers a cost-effective alternative to optimize energy generation under partial shadings in the system rather than relying solely on complex and expensive control systems [16]. The reconfiguration proceeds with the physical rearrangement of the connections or positions of the connected modules to minimize shading-induced mismatches and extract maximum available power from the array. The PV array reconfigurations are classified into two categories based on the operation i.e., static and dynamic.

Static array reconfiguration technique involves fixed and predetermined modification in the physical arrangement of modules, typically based on a priori knowledge of shading patterns [17]. These reconfigurations are implemented to improve power generation of the array by mitigating partial shading effects through shade dispersion [18]. Also, these are cost-effective and easier to manage, as they do not require sophisticated tracking or sensing systems. Also, the static techniques can be particularly useful in cases where shading patterns are known or stable, allowing for improved power generation without the need for continuous rearrangement. In [19], a triple X Sudoku method has been proposed that physically changes the modules' position, tested over twelve shading, and found more effective than other techniques. Another static technique based on an addition progression structure has been proposed in [20] whose performance surpasses the conventional methods with a maximum reduction of 38.36% in mismatch power loss, and 1.62 more fill factor than the total cross tied (TCT) method. A four-square (FS) reconfiguration has been proposed, tested under static and dynamic shading scenarios and resulted in a power enhancement of 38.016% in the existence of random failed modules [21]. Similarly, a henon map (HM) reconfiguration has been proposed, tested using 9×9, 8×8, 4×4, 3×5 and 4×3 PV arrays under distinct shading patterns, compared with existing techniques and found to have a maximum power enhancement of 24.17%, 25.65%, and 47.81% for various shading cases of 9×9, 8×8, and 4×4 PV arrays, respectively [22]. Some other static reconfigurations include Sudoku [23], Futoshiki [24], Magic Square (MS) [25], Competence Square (CS) [26], SD-PAR [27], Odd-Even (OE) [28], electrical reconfiguration (ER) [29], ancient Chinese (AC) [30], modified Sudoku (MOS) [31], hyper Sudoku (HS) [32], Chaos Map (CM) [33], fixed electrical reconfiguration (FER) [34], Successive rotation [35], Calcudoku [36], Ramanujan reconfiguration [37], skyscraper [38], etc. that can enhance the power generation of PV arrays during shading. However, adaptability to rapidly changing or unpredictable partial shading conditions, inefficiency under variable shading, complex wiring, limited application to arbitrary PV arrays due to square puzzle pattern concepts, improper shade dispersion, and reliability are some of the major drawbacks of static techniques while implementing in real-time scenarios.

Dynamic reconfiguration is the most reliable and efficient method of extracting possible maximum power from the PV arrays during partial shading that works by changing the electrical connection of modules based on the partial shading scenario [39]. The electrical reconnection is typically done through a switching matrix system that works based on data collected from sensors, weather forecasts, or algorithms that continuously monitor shading patterns [40]. Also, this methodology is highly flexible and responsive as compared to static methods allowing better adaption to varying and unpredictable partial shading scenarios. An improved Pelican optimization algorithm for switching matrix is proposed in [41] that improved the power generation of PV array by up to 30% during short and wide shading cases. A dynamic leader based collective intelligence reconfiguration algorithm has been proposed in [42] which is found to be effective in enhancing the power output of arrays and reducing the peaks in the power-voltage (P-V) curves during partial shading. A permutation-combination (P-C) reconfiguration is proposed, tested in 4 × 4, 6 × 4 and 9 × 9 and found to have an enhanced efficiency of up to 1.67% and reduced losses by 7-8% during shading [43]. Some other dynamic algorithms include genetic algorithm (GA) [44], particle swarm optimization (PSO) [45], African vultures optimization (AVO) [46], modified harris hawks optimizer (MHHO) [47], dragonfly (DF) [48], honey badger (HB) [49], Munkres assignment (MA) [50], grey wolf optimization (GWO) [51], firefly (FF) [52], etc. that have the similar potential of power enhancement in PV arrays during shading. However, complex algorithms, slow convergence, high computational loads,

improper parameter tuning, scalability, etc. are some of the major drawbacks of these techniques.

So, in this paper, a simple harmony search (HS) algorithm for the switching matrix of the dynamic array reconfiguration has been proposed for power enhancement during partial shading. The proposed algorithm exhibits advantages such as simplicity, faster convergence, lower computational load, robust, stability, less sensitive to premature convergence, adaptability, fewer complex parameters, efficiency, and wide application to arbitrary array sizes as compared to the other techniques. The proposed HS technique has been tested using three array sizes of 5 × 5, 9 × 9 and 9 × 5 under numerous partial shading cases and compared with series-parallel (SP), total-cross-tied (TCT), Sudoku [23], Futoshiki [24], Magic Square (MS) [25], Competence Square (CS) [26], SD-PAR [27], Odd-Even (OE) [28], electrical reconfiguration (ER) [29], ancient Chinese (AC) [30], modified Sudoku (MOS) [31], hyper Sudoku (HS) [32], Chaos Map (CM) [33] and FER [34] in MATLAB platform. Later on, comparison of the proposed technique with various dynamic algorithms such as genetic algorithm (GA) [30], particle swarm optimization (PSO) [40], African vultures optimization (AVO) [41], modified Harris hawks optimizer (MHHO) [42], dragonfly (DF) [43], honey badger (HB) [44], Munkres assignment (MA) [45], grey wolf optimization (GWO) [46] and firefly (FF) [47] techniques has been carried out under different shading cases. The comparison is done using generated P-V curves, power output, loss, efficiency, enhancement, and available power deviation.

The rest portions of the paper include system description, comparison parameters, and existing techniques in Section II, description of harmony search algorithm and implementation in arrays in Section III, evaluation of different arrays under shading in Section IV followed by conclusion in Section V.

II. SYSTEM DESCRIPTION, COMPARISON PARAMETERS AND EXISTING TECHNIQUES

In this section, the description of the PV arrays and existing reconfiguration techniques for arrays have been explained.

A. SYSTEM DESCRIPTION

In this study, three sizes of PV arrays i.e., 5 × 5, 9 × 9, and 9 × 5 have been used for analysis under partial shading which as formed by connecting numerous same-rated modules. The rating of the modules used in the study at standard testing conditions (STC) of 1000W/m^2 (solar irradiance) and 25°C (operating temperature) has been described below:

Maximum Rated Power Output (P_R): 325W
Maximum Rated Voltage Output (V_R): 37.80V
Maximum Rated Current Output (I_R): 8.60A
Open-circuit Voltage (V_{OC}): 46.60V
Short-Circuit Current (I_{SC}): 9.20A
Irradiance Receiving Area (A): 1.696m^2

The total power output of 5 × 5. 9 × 9 and 9 × 5 arrays under STC have been noted as 8.125kW, 26.325kW and 14.625kW respectively. However, to meet the real-time conditions, the analysis has been conducted under nominal operating cell temperature (NOCT) with solar irradiance and temperature of 800W/m^2 and 50°C (field condition). Hence, the total power outputs of 5 × 5, 9 × 9, and 9 × 5 arrays at NOCT have been noted as 6.62kW, 21.56kW, and 12.30kW respectively.

B. COMPARISON PARAMETERS

The performance of the PV arrays under partial shading is evaluated using various comparative parameters like power loss, efficiency, power enhancement, actual power deviation, and peak count whose mathematical expressions have been explained below.

The power loss is the measure of lost power due to the occurrence of shading in the array and can be measured from the difference between the power output under normal (P_N) and shading (P_{G^*}) where 'C' indicates the configuration type and given by

$$Power\ Loss(in\%) = [(P_N - P_{GC})/P_N]^*100 \quad (1)$$

The power enhancement of any array configuration than the conventional series-parallel (SP) connection is calculated using equation (2) where 'P_{SP}' denotes the power output of the SP connection.

$$Power\ Enhancement(\%) = [(P_{GC} - P_{SP})/P_{SP}]^*100 \quad (2)$$

The actual power deviation is the difference between the total power available (P_A) in the array and generated power given by

$$Actual\ Power\ Deviation(\%) = [(P_A - P_{GC})/P_A]^*100 \quad (3)$$

The efficiency is the ratio of input and output of the array that can be calculated using equation (4) where 'G' and 'A' reflect the solar irradiance and area of module respectively.

$$Efficiency(\%) = [P_G{}^*/(G^*A)]^*100 \quad (4)$$

The peak count is the measure of total number of power peaks that exist in the P-V curves of the array during shading.

C. EXISTING PV ARRAY RECONFIGURATION TECHNIQUES

The PV arrays are generally connected in series-parallel (SP) connection as shown in FIGURE 1 (a) in which modules are connected in string and such strings are connected in parallel. Later on, the SP connection is modified by connecting ties across the modules' junctions to enhance array performance during partial shading and named total cross tied (TCT) as shown in FIGURE 1 (b).

However, the above configurations fail to generate higher power output during partial shading and hence, several other reconfiguration techniques have been adopted to enhance the overall power generation of the system.

These reconfiguration techniques work on the principle of shade dispersion to minimize the row current difference that enhances the power generation of the array. FIGURE 2 shows various reconfiguration techniques for 5 × 5 arrays that include TCT, Sudoku [23], Futoshiki [24], Magic Square

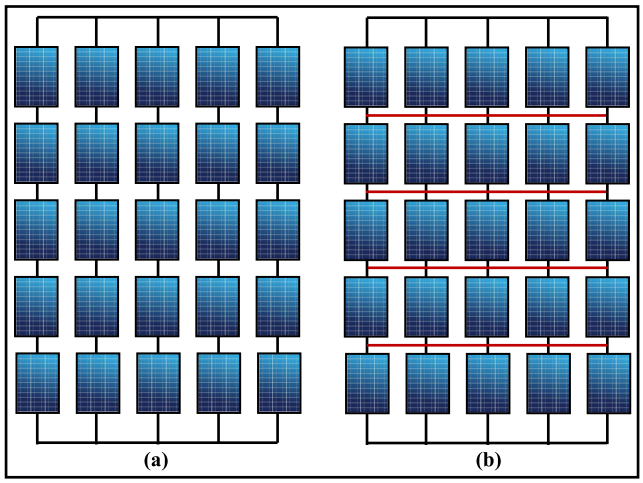

FIGURE 1. Conventional PV array configurations. (a) Series-Parallel (SP), and (b) Total Cross Tied (TCT).

(MS) [25], Competence Square (CS) [26], SD-PAR [27], and Odd-Even [28]. Similarly, FIGURE 3 shows reconfiguration techniques for 9 × 9 PV arrays that consist of TCT, ER [29], ancient Chinese (AC) [30], Sudoku [23], modified Sudoku (MOS) [31], hyper Sudoku (HS) [32] and Chaos Map (CM) [33]. These techniques can be implemented in the PV arrays by either changing the electrical connections or physical positions of the modules and proved to be effective in various studies. So, in this paper, the above techniques have been considered to compare the performance of the proposed technique under partial shading along with the conventional SP and TCT connections. Additionally, various dynamic techniques such as genetic algorithm (GA) [39], particle swarm optimization (PSO) [40], African vultures optimization (AVO) [41], modified Harris hawks optimizer (MHHO) [42], dragonfly (DF) [43], honey badger (HB) [44], Munkres assignment (MA) [45], grey wolf optimization (GWO) [46] and firefly algorithm (FF) [47] have been used for the comparison with 9 × 9 PV arrays. Also, FER [34] has been used for the comparison with the proposed technique in a 9 × 5 array along with SP and TCT.

III. HARMONY SEARCH (HS) ALGORITHM BASED SWITCHING MATRIX FOR RECONFIGURATION

In this section, a simple algorithm based on harmony search (HS) optimization for switching matrix which can efficiently disperse the shading, minimize the current difference among rows, and effectively improve the power generation of the PV array during partial shading has been proposed.

A. BACKGROUND

The Harmony Search (HS) algorithm is a nature-inspired optimization technique skillfully employed to tackle intricate optimization challenges invented in 2001 by Geem, Kim, and Loganathan. The HS algorithm is inspired by the process of musicians finding harmonious solutions while improvising. It mimics the musical improvisation process by searching for optimal solutions in a problem space. In the HS algorithm, potential solutions are represented as the ''harmonies,'' and these harmonies are improved iteratively to find the best possible solution by adjusting and combining elements from different harmonies, much like a musician blends musical notes to create a harmonious melody.

B. MATHEMATICAL MODELS FOR HARMONY SEARCH (HS) ALGORITHM

Different mathematical models are used in the HS algorithm for improvision, replacement, and harmony update. Equation 5 has been used to initialize a population of random solutions (i.e., harmonies) within the problem's search space.

$$x_{i,i} = l_i + rand \times (u_i - l_i) \, for \\ i = 1, 2, 3, \ldots, N \; and \; j = 1, 2, 3, \ldots, d \qquad (5)$$

where, l_j, $u_{j,}$ and j denote the lower bound, upper bound, and decision variable respectively.

Then, the fitness value for each harmony is calculated based on the objective function that indicates how good it is to the problem's objective. The harmony memory is used to keep a record of the best harmonies discovered so far which is updated in each iteration with best harmonies.

Step 1 (Improvision): By merging the elements from the population's previous harmonies, new harmony is created in the HS which is produced using various operators including Pitch Adjustment Rate (PAR), Pitch Memory Consideration, Randomization (0,1) and Harmony Memory Consideration Rate (HMCR). These search operators aim to retain diversity while efficiently searching the search space. The HMCR is harmony memory component retrieval probability. The range [0 1] is the normal distribution of a random integer (rand). Equation (6) is used to generate a new harmony at random if (rand > HMCR).

$$x_{new,j} = l_j + rand \times \left(u_j - l_j\right) \qquad (6)$$

If (rand ≤ HMCR), then one harmony is randomly selected using equation (7).

$$x_{new,j} = x_{k,j} \quad where \; 1 \; \leq k \leq N \qquad (7)$$

Step 2 (Pitch Adjustment Rate (PAR)): In HS algorithm, a pitch adjustment strategy is used to escape from local optima. PAR value ranges from 0 to 1, with 0 denoting poor pitch adjustment and 1 denoting good pitch adjustment. If (rand ≤ PAR), apply pitch adjustment bandwidth to modify x_j using equation (8).

$$x_{new,j} = x_{new,j} + bw \times (rand - 0.5) \times \left|u_j - l_j\right| \qquad (8)$$

where rand is any random number between 0 and 1, and bw is generation's bandwidth. A random integer is generated from [-0.5 0.5] by the equation (rand-0.5).

Step 3 (Replacement): Using an objective function, the fitness value of a newly created harmony is calculated. The new harmony is compared to the worst harmony in the harmony

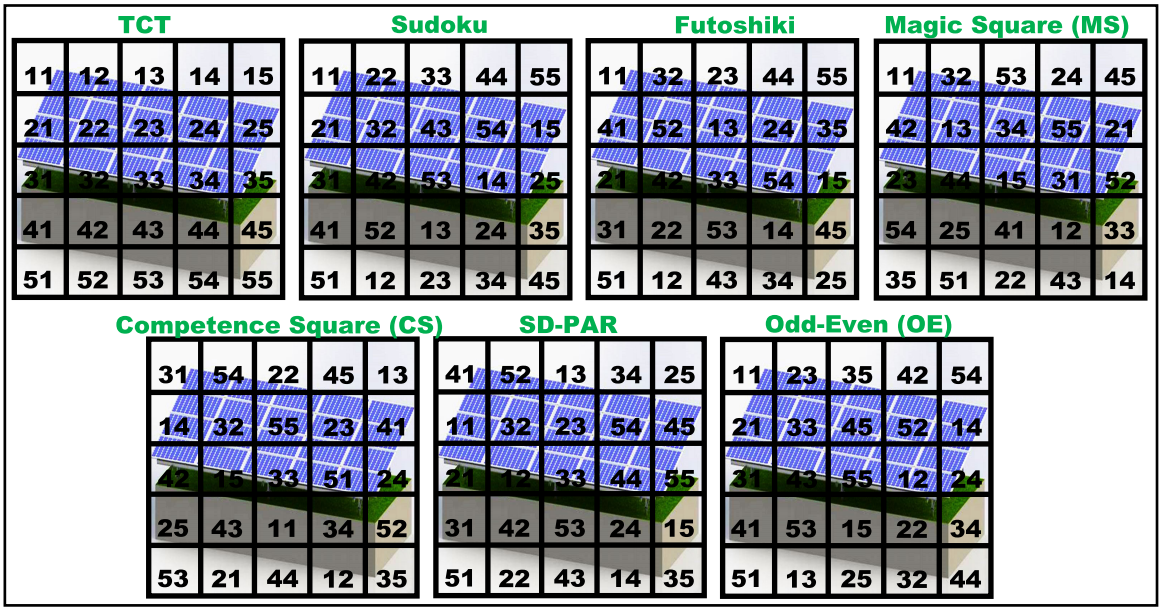

FIGURE 2. Static reconfiguration techniques used for comparison with the proposed technique for 5 × 5 PV arrays.

memory. If the new harmony's fitness value is higher than that of the preceding harmony, it is replaced.

Step 4 (Output): Best harmony in the harmony memory is returned as the optimal solution.

C. HARMONY SEARCH RECONFIGURATION (HSR) ALGORITHM FOR PV ARRAY RECONFIGURATION

During partial shading, the arrays receive multiple irradiance levels as a result, modules generate different current outputs causing a mismatch. The main aim of array reconfiguration is to reduce the mismatch by reducing the difference in current among the rows of the PV array. A general model of an array reconfiguration consists of a PV array with MxN modules connected in the TCT configuration, a switching matrix (SM) system that performs electrical connection switching among modules, and an algorithm to calculate optimal configuration based on the shading scenario and perform the switching in the switching matrix system as shown in FIGURE 4 (a).

The HSR algorithms take the real-time irradiance data of the modules as input, calculate the current outputs of each module followed by each row, then evaluate the difference in current between rows, perform reconfiguration operation, and deliver the optimal switching pattern for electrical re-configuration among modules for higher power generation. FIGURE 4 (b) shows the flowchart involved in the proposed HS algorithm for array reconfiguration and the pseudo-code has been given below:

The implementation of the proposed HS algorithm in PV array reconfiguration involves a series of key steps given below:

Step 1 (Parameter Initialization): The initialization of the parameters involved in the HS algorithm such as harmony memory size (HMS), pitch adjustment rate (PAR), and maximum iteration is set as 20, 0.3, and 500 respectively.

Step 2 (Data Initialization): The algorithm takes the array size (row x column) and real-time solar irradiance data of individual modules.

Step 3 (Calculation): The algorithm calculates the current, of individual module and array voltage using equations (9) and (10) respectively.

$$I_{Mij} = \left(\frac{S_{ij}}{S_o}\right) \times I_M \tag{9}$$

where, I_M, i, j, S_{ij} and S_o denote the maximum current of the module at STC, row index, column index, irradiance received by i^{th} row and j^{th} column, and standard irradiance level (1000W/m^2) respectively.

$$V_a = \sum_{k=2}^{k=r} V_{mk} \tag{10}$$

where V_a and V_{mk} represent the array voltage and voltage of the k^{th} row respectively.

Step 4 (Objective Function): The objective function of the algorithm has been declared as

$$MaximizeF(i) = \sum(p) + \left(\frac{W_e^2}{E_r}\right) + \left(W_p^2 \times P_a\right) \tag{11}$$

where W_e and W_p are the weights associated with PV array maximum power (P_a) and sum of error between maximum row current and individual row current (E_r).

Step 5: The algorithm evaluates the initial harmonies or array configuration and its performance using the objective function and stores it in the harmony memory.

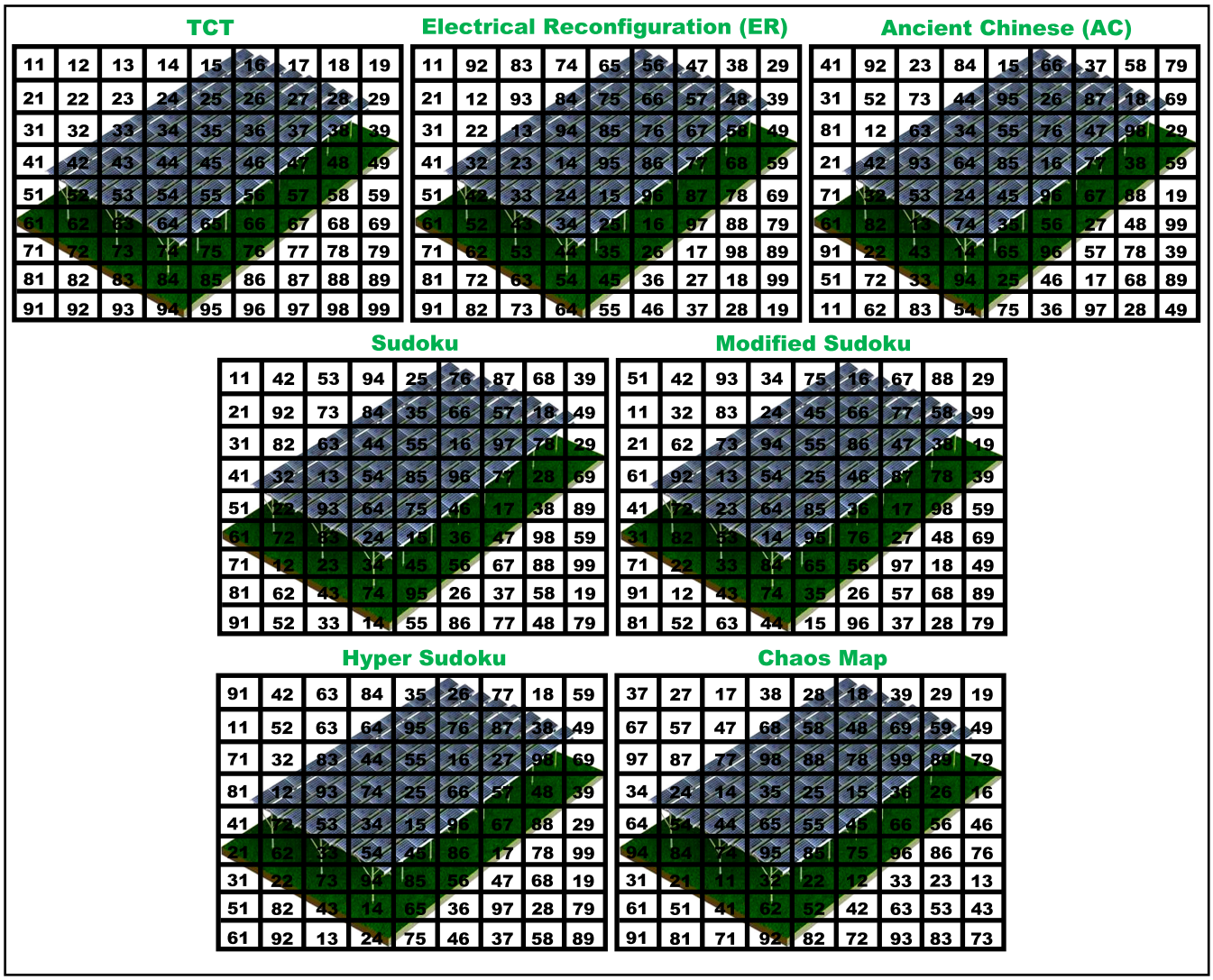

FIGURE 3. Static reconfiguration techniques used for comparison with the proposed technique for 9 × 9 PV arrays.

Step 6: The algorithm starts the iterative harmony search process where new configurations are generated by swapping the modules in column way to meet the objective function.

Step 7: The algorithm uses objective function to evaluate the new harmony or configuration.

Step 8: The algorithm compares the power output of the newly generated harmony or configuration with the existing harmony in the memory and replaces it with a new harmony value if higher power output is noted.

Step 9: The algorithm repeats the iteration process until it gets higher power with reduced difference between row currents of the PV array.

Step 10: The algorithm continuously monitors the array irradiance level and operates if multiple irradiance levels are detected in the PV array.

It is to be noted that the algorithm remains ideal along with the switching matrix system when no multiple irradiance or partial shading is detected.

D. SWITCH COUNT AND WIRE LENGTH ESTIMATION

As mentioned previously, the HSR technique utilizes the TCT connection along with a switching matrix system, hence the total number of switches (T_{SW}) required in the proposed system can be estimated as

$$S_{HSR} = 2 \times M \times N \tag{12}$$

where, 'M' and 'N' represent the row and column counts of the PV array respectively. The proposed switching matrix system requires less switches as compared to conventional techniques with a higher count of '*[2xN(MxN)+ M(M+1)-2]*'.

In addition, the wire length (L_{HSR}) of the PV array with the HSR can be estimated as

$$L_{HSR} = T_{PV} \times \sqrt{V^2 + H^2} \tag{13}$$

where, 'T_{PV}', 'V' and 'H' denote the total number of modules in the PV array, vertical and horizontal distance between

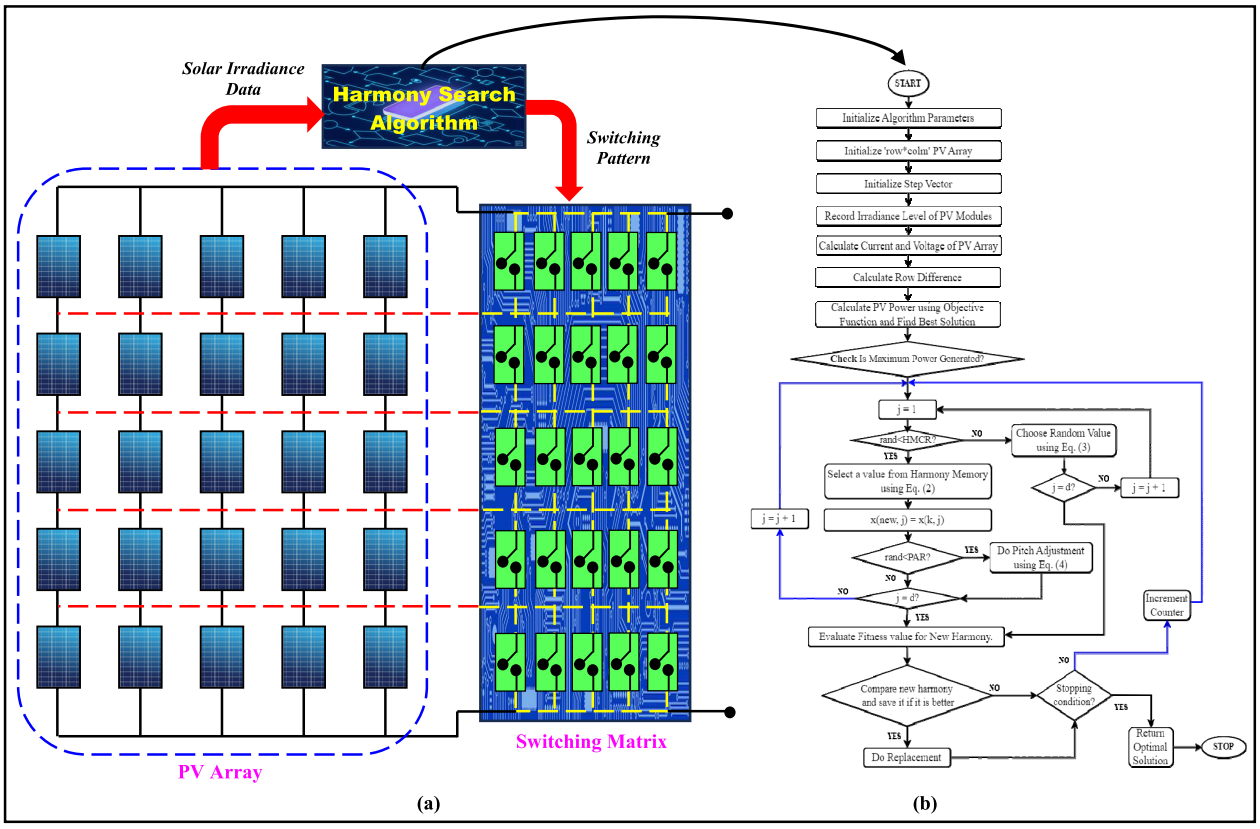

FIGURE 4. Architecture for reconfiguration. (a) 5 × 5 array with switching matrix, and (b) Flowchart of Harmony Search Reconfiguration (HSR) algorithm.

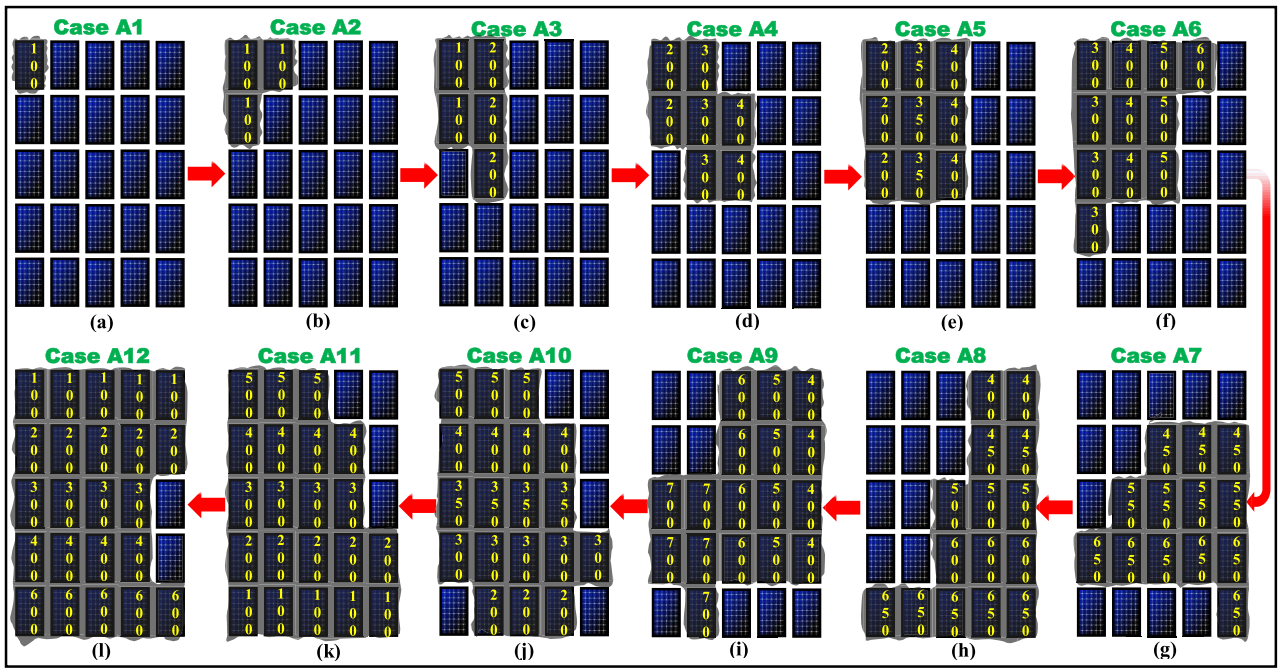

FIGURE 5. Partial shading case (a) A1, (b) A2, (c) A3, (d) A4, (e) A5, (f) A6, (g) A7, (h) A8, (i) A9, (j) A10, (k) A11 and (l) A12 for 5×5 PV arrays (digit represent irradiance values in W/m^2 and normal modules receiving 800W/m^2).

connected modules respectively. It is to be noted that the PV array is connected to the switching matrix system that consist of switches and may require additional wires for connection.

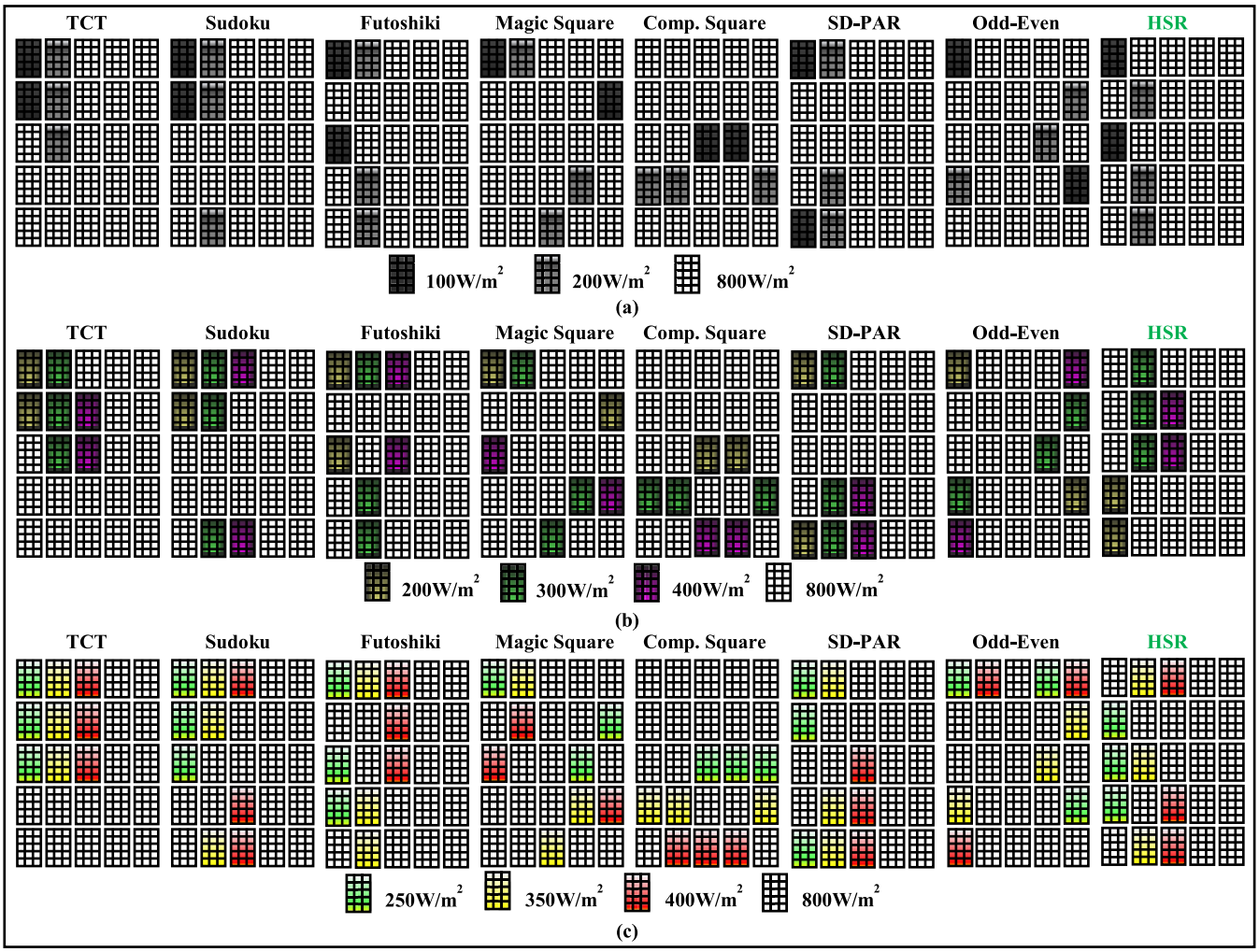

FIGURE 6. Dispersion of irradiance levels by different array reconfiguration techniques and proposed HSR during shading case (a) A3, (b) A4, and (c) A5.

IV. EVALUATION OF PV ARRAYS UNDER PARTIAL SHADING

In this study, two symmetrical PV arrays of sizes of 5×5 and 9×9 along with an unsymmetrical 9×5 PV array have been considered to show the effectiveness of the proposed HSR as compared to the conventional and existing techniques during partial shading. The entire analysis has been conducted under NOCT taking 800W/m^2 irradiance and 50°C temperature as normal or unshaded scenario.

A. ANALYSIS USING 5 × 5 PV ARRAY

The proposed HSR has been implemented to a 5×5 PV array and compared with SP, TCT, Sudoku [23], Futoshiki [24], Magic Square (MS) [25], Competence Square (CS) [26], SD-PAR [27] and Odd-Even (OE) [28] techniques under twelve distinct shading cases as shown in FIGURE 5.

The maximum power output of all the array techniques has been noted as 6.62kW during normal scenario at NOCT. The shading cases (FIGURE 5) considered in the study initially start with the shading of one module (4% shading) to twenty-three modules (92%) and the performance of each technique has been investigated and compared with the proposed HSR.

1) CASE A1 (4% SHADING)

The shading case A1 has been presented in FIGURE 5 (a) where one module received a lower irradiance of 100W/m^2. The P-V curves in FIGURE 7 (a) show that all techniques have equal characteristics and power output of 5.56kW with 16.01% power loss, -0.89% deviation from available power (5.61kW as total available power), 16.45% efficiency, and 2 peaks.

2) CASE A2 (12% SHADING)

During this case (FIGURE 5 (b)), two modules of column-1 and one module of column-2 receive 100 W/m^2. The P-V graphs have been shown in FIGURE 7 (b) and it has been found that HSR, OE, SD-PAR, MS, Futoshiki, and Sudoku

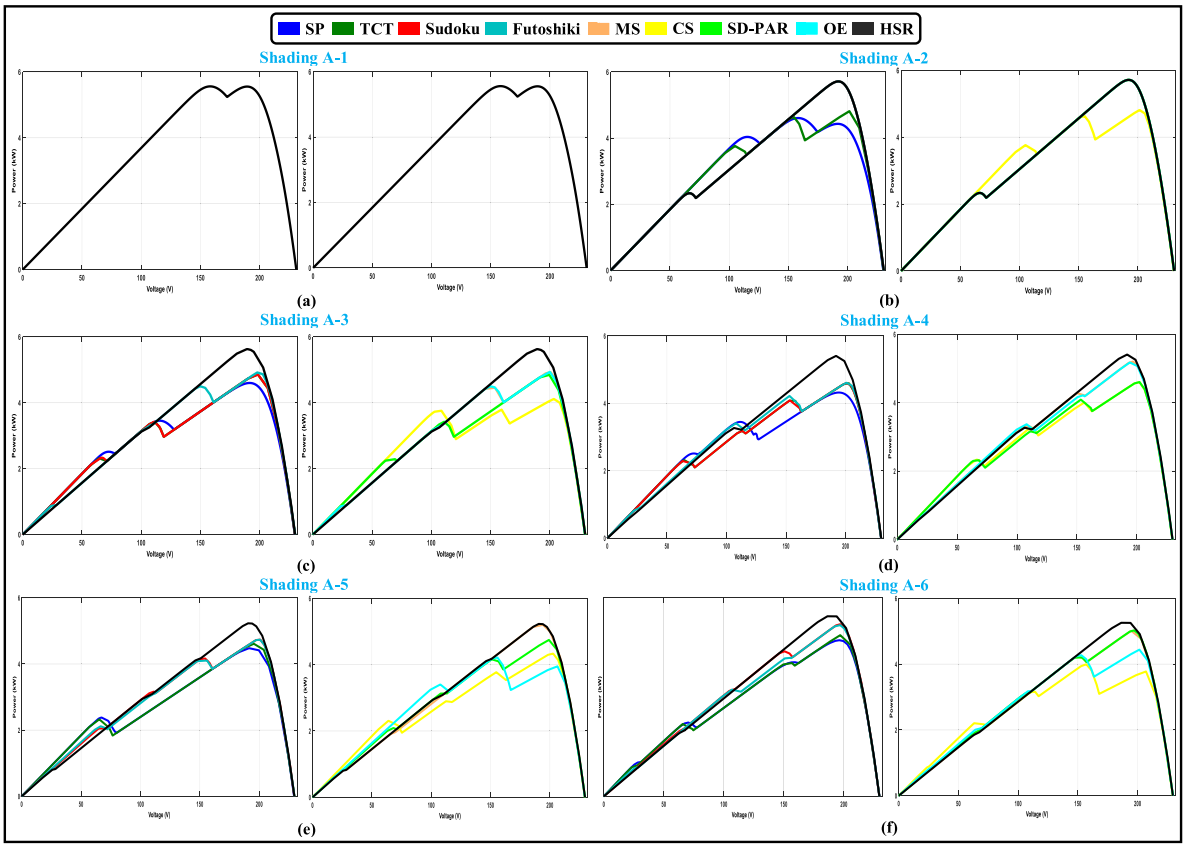

FIGURE 7. P-V curves of different PV array configuration techniques during shading cases (a) A1, (b) A2, (c) A3, (d) A4, (e) A5, and (f) A6.

have equal power outputs of 5.71kW whereas CS and TCT generated the same powers of 4.81kW. The power output in the SP connection has been noted to be the lowest.

3) CASE A3 (20% SHADING)

During this case, as shown in FIGURE 5 (c), two modules of column-1 (100W/m^2) and three modules of column-2 (200 W/m^2) are receiving different irradiance levels as compared to others (800W/m^2).

The dispersion of shade by different techniques has been presented in FIGURE 6 (a) and the calculation of row currents of different techniques are as follows.

For the TCT connection, the current output from all the five rows ($I_{Row1(TCT)}$ to $I_{Row5(TCT)}$) of the PV array has been calculated as

$$I_{Row1(TCT)} = (100/1000)I_r + (200/1000)I_r + 3(800/1000)I_r = 0.1I_r + 0.2I_r + 3^*(0.8)I_r = 2.7I_r \quad (14)$$

$$I_{Row2(TCT)} = 0.1I_r + 0.2I_r + 3^*(0.8)I_r = 2.7I_r \quad (15)$$

$$I_{Row3(TCT)} = 0.8I_r + 0.2I_r + 3^*(0.8)I_r = 3.4I_r \quad (16)$$

$$I_{Row4(TCT)} = I_{Row5(TCT)} = 5^*(0.8)I_r = 4.0I_r \quad (17)$$

For the Sudoku technique, the current output from all five rows ($I_{Row1(Sud)}$ to $I_{Row5(Sud)}$) of the array has been calculated as

$$I_{Row1(Sud)} = 0.1I_r + 0.2I_r + 3^*(0.8)I_r = 2.7I_r \quad (18)$$

$$I_{Row2(Sud)} = 0.1I_M + 0.2I_r + 3^*(0.8)I_r = 2.7I_r \quad (19)$$

$$I_{Row3(Sud)} = I_{R4(Sud)} = 5^*(0.8)I_r = 4.0I_r \quad (20)$$

$$I_{Row5(Sud)} = 0.8I_r + 0.2I_r + 3^*(0.8)I_r = 3.4I_r \quad (21)$$

For the Futoshiki technique, the current output from all five rows ($I_{Row1(Fut)}$ to $I_{Row5(Fut)}$) of the PV array has been calculated as

$$I_{Row1(Fut)} = 0.1I_r + 0.2I_r + 3^*(0.8)I_r = 2.7I_M \quad (22)$$

$$I_{Row2(Fut)} = 5^*(0.8)I_r = 4.0I_r \quad (23)$$

$$I_{Row3(Fut)} = 0.1I_r + 4^*(0.8)I_r = 3.3I_r \quad (24)$$

$$I_{Row4(Sud)} = I_{Row5(Sud)} = 0.8I_r + 0.2I_r + 3^*(0.8)I_r = 3.4I_r \quad (25)$$

For the MS technique, the current output from all five rows ($I_{Row1(MS)}$ to $I_{Row5(MS)}$) of the array has been calculated as

$$I_{Row1(MS)} = 0.1I_r + 0.2I_r + 3^*(0.8)I_r = 2.7I_r \quad (26)$$

$$I_{Row2(MS)} = 4^*(0.8)I_r + 0.1I_r = 3.3I_r \quad (27)$$

$$I_{Row3(MS)} = 5^*(0.8)I_r = 4.0I_r \quad (28)$$

$$I_{Row4(MS)} = I_R5(MS) = 0.2I_r + 4^*(0.8)I_r = 3.4I_r \quad (29)$$

TABLE 1. Theoretical calculation of current, voltage, and power of different techniques during cases A1 to A4.

Partial Shading A1																
TCT				**Sudoku**				**Futoshiki**				**MS**				
Row	***I***	***V***	***P***	***Row***	***I***	***V***	***P***	***Row***	***I***	***V***	***P***	***Row***	***I***	***V***	***P***	
Row 1	3.3I_r	5V_r	16.50P_r	Row 1	3.3I_r	5V_r	16.50P_r	Row 1	3.3I_r	5V_r	16.50P_r	Row 1	3.3I_r	5V_r	16.50P_r	
Row 2	4.0 I_r	4V_r	16.00P_r	Row 2	4.0I_r	4V_r	16.00P_r	Row 2	4.0I_r	4V_r	16.00P_r	Row 2	4.0I_r	4V_r	16.00P_r	
Row 3	4.0 I_r	3V_r	12.00P_r	Row 3	4.0I_r	3V_r	12.00P_r	Row 3	4.0I_r	3V_r	12.00P_r	Row 3	4.0I_r	3V_r	12.00P_r	
Row 4	4.0 I_r	2V_r	8.00P_r	Row 4	4.0I_r	2V_r	8.00P_r	Row 4	4.0I_r	2V_r	8.00P_r	Row 4	4.0I_r	2V_r	8.00P_r	
Row 5	4.0 I_r	V_r	4.00P_r	Row 5	4.0I_r	V_r	4.00P_r	Row 5	4.0I_r	V_r	4.00P_r	Row 5	4.0I_r	V_r	4.00P_r	
CS				**SD-PAR**				**OE**				**HSR**				
Row	***I***	***V***	***P***	***Row***	***I***	***V***	***P***	***Row***	***I***	***V***	***P***	***Row***	***I***	***V***	***P***	
Row 1	3.3I_r	5V_r	16.50P_r	Row 1	3.3I_r	5V_r	16.50P_r	Row 1	3.3I_r	5V_r	16.50P_r	Row 1	3.3I_r	5V_r	16.50P_r	
Row 2	4.0I_r	4V_r	16.00P_r	Row 2	4.0I_r	4V_r	16.00P_r	Row 2	4.0I_r	4V_r	16.00P_r	Row 2	4.0I_r	4V_r	16.00P_r	
Row 3	4.0I_r	3V_r	12.00P_r	Row 3	4.0I_r	3V_r	12.00P_r	Row 3	4.0I_r	3V_r	12.00P_r	Row 3	4.0I_r	3V_r	12.00P_r	
Row 4	4.0I_r	2V_r	8.00P_r	Row 4	4.0I_r	2V_r	8.00P_r	Row 4	4.0I_r	2V_r	8.00P_r	Row 4	4.0I_r	2V_r	8.00P_r	
Row 5	4.0I_r	V_r	4.00P_R	Row 5	4.0I_r	V_r	4.00P_r	Row 5	4.0I_r	V_r	4.00P_r	Row 5	4.0I_r	V_r	4.00P_r	
Partial Shading A2																
TCT				**Sudoku**				**Futoshiki**				**MS**				
Row	***I***	***V***	***P***	***Row***	***I***	***V***	***P***	***Row***	***I***	***V***	***P***	***Row***	***I***	***V***	***P***	
Row 1	2.6I_r	5V_r	13.00P_r	Row 1	3.3I_r	5V_r	16.50P_r	Row 1	3.3I_r	5V_r	16.50P_r	Row 1	3.3I_r	5V_r	16.50P_r	
Row 2	3.3I_r	4V_r	13.20P_r	Row 2	3.3I_r	4V_r	13.20P_r	Row 3	3.3I_r	4V_r	13.20P_r	Row 2	3.3I_r	4V_r	13.20P_r	
Row 3	4I_r	3V_r	12.00P_r	Row 5	3.3I_r	3V_r	9.90P_r	Row 5	3.3I_r	3V_r	9.90P_r	Row 4	3.3I_r	3V_r	9.90P_r	
Row 4	4I_r	2V_r	8.00P_r	Row 3	4I_r	2V_r	8.00P_r	Row 2	4I_r	2V_r	8.00P_r	Row 3	4I_r	2V_r	8.00P_r	
Row 5	4I_r	V_r	4.00P_r	Row 4	4I_r	V_r	4.00P_r	Row 4	4I_r	V_r	4.00P_r	Row 5	4I_r	V_r	4.00P_r	
CS				**SD-PAR**				**OE**				**HSR**				
Row	***I***	***V***	***P***	***Row***	***I***	***V***	***P***	***Row***	***I***	***V***	***P***	***Row***	***I***	***V***	***P***	
Row 3	2.6I_r	5V_r	13.00P_r	Row 1	3.3I_r	5V_r	16.50P_r	Row 1	3.3I_r	5V_r	16.50P_r	Row 1	3.3I_r	5V_r	16.50P_r	
Row 4	3.3I_r	4V_r	13.20P_r	Row 4	3.3I_r	4V_r	13.20P_r	Row 3	3.3I_r	4V_r	13.20P_r	Row 3	3.3I_r	4V_r	13.20P_r	
Row 1	4I_r	3V_r	12.00P_r	Row 5	3.3I_r	3V_r	9.90P_r	Row 4	3.3I_r	3V_r	9.90P_r	Row 4	3.3I_r	3V_r	9.90P_r	
Row 2	4I_r	2V_r	8.00P_r	Row 2	4I_r	2V_r	8.00P_r	Row 2	4I_r	2V_r	8.00P_r	Row 2	4I_r	2V_r	8.00P_r	
Row 5	4I_r	V_r	4.00P_r	Row 3	4I_r	V_r	4.00P_r `	Row 5	4I_r	V_r	4.00P_R	Row 5	4I_r	V_r	4.00P_r	
Partial Shading A3																
TCT				**Sudoku**				**Futoshiki**				**MS**				
Row	***I***	***V***	***P***	***Row***	***I***	***V***	***P***	***Row***	***I***	***V***	***P***	***Row***	***I***	***V***	***P***	
Row 1	2.7I_r	5V_r	13.50P_r	Row 1	2.7I_r	5V_r	13.50P_r	Row 1	2.7I_r	5V_r	13.50P_r	Row 1	2.7I_r	5V_r	13.50P_r	
Row 2	2.7I_r	4V_r	10.80P_r	Row 2	2.7I_r	4V_r	10.80P_r	Row 3	3.3I_r	4V_r	13.20P_r	Row 2	3.3I_r	4V_r	13.20P_r	
Row 3	3.4I_r	3V_r	10.20P_r	Row 5	3.4I_r	3V_r	10.20P_r	Row 4	3.4I_r	3V_r	10.20P_r	Row 4	3.4I_r	3V_r	10.20P_r	
Row 4	4I_r	2V_r	8.00P_r	Row 3	4I_r	2V_r	8.00P_r	Row 5	3.4I_r	2V_r	6.80P_r	Row 5	3.4I_r	2V_r	6.80P_r	
Row 5	4I_r	V_r	4.00P_r	Row 4	4I_r	V_r	4.00P_r	Row 2	4I_r	V_r	4.00P_r	Row 3	4I_r	V_r	4.00P_r	
CS				**SD-PAR**				**OE**				**HSR**				
Row	***I***	***V***	***P***	***Row***	***I***	***V***	***P***	***Row***	***I***	***V***	***P***	***Row***	***I***	***V***	***P***	
Row 4	2.2I_r	5V_r	11.00P_r	Row 1	2.7I_r	5V_r	13.50P_r	Row 4	2.7I_r	5V_r	13.50P_r	Row 1	3.3I_r	5V_r	16.50P_r	
Row 3	2.6I_r	4V_r	10.40P_r	Row 5	2.7I_r	4V_r	10.80P_r	Row 1	3.3I_r	4V_r	13.20P_r	Row 3	3.3I_r	4V_r	13.20P_r	
Row 1	4I_r	3V_r	12.00P_r	Row 4	3.4I_r	3V_r	10.20P_r	Row 2	3.4I_r	3V_r	10.20P_r	Row 5	3.3I_r	3V_r	9.90P_r	
Row 2	4I_r	2V_r	8.00P_r	Row 2	4I_r	2V_r	8.00P_r	Row 3	3.4I_r	2V_r	6.80P_r	Row 2	3.4I_r	2V_r	6.80P_r	
Row 5	4I_r	V_r	4.00P_r	Row 3	4I_r	V_r	4.00P_r	Row 5	4I_r	V_r	4.00P_r	Row 4	3.4I_r	V_r	3.40P_r	
Partial Shading A4																
TCT				**Sudoku**				**Futoshiki**				**MS**				
Row	***I***	***V***	***P***	***Row***	***I***	***V***	***P***	***Row***	***I***	***V***	***P***	***Row***	***I***	***V***	***P***	
Row 1	2.9I_r	5V_r	14.50P_r	Row 1	2.5I_r	5V_r	12.50P_r	Row 1	2.9I_r	5V_r	14.50P_r	Row 1	2.9I_r	5V_r	14.50P_r	
Row 2	2.9I_r	4V_r	11.60P_r	Row 2	2.5I_r	4V_r	10.00P_r	Row 3	3I_r	4V_r	12.00P_r	Row 4	3.1I_r	4V_r	12.40P_r	
Row 3	3.1I_r	3V_r	9.30P_r	Row 5	3.5I_r	3V_r	10.50P_r	Row 5	3.1I_r	3V_r	9.30P_r	Row 5	3.1I_r	3V_r	9.30P_r	
Row 4	3.6I_r	2V_r	7.20P_r	Row 3	4I_r	2V_r	8.00P_r	Row 4	3.5I_r	2V_r	7.00P_r	Row 2	3.4I_r	2V_r	6.80P_r	
Row 5	4I_r	V_r	4.00P_r	Row 4	4I_R	V_r	4.00P_r	Row 2	4I_r	V_r	4.00P_r	Row 3	4I_r	4V_R	4.00P_r	
CS				**SD-PAR**				**OE**				**HSR**				
Row	***I***	***V***	***P***	***Row***	***I***	***V***	***P***	***Row***	***I***	***V***	***P***	***Row***	***I***	***V***	***P***	
Row 4	2.5I_r	5V_r	12.50P_r	Row 1	2.5I_r	5V_r	12.50P_r	Row 4	2.9I_r	5V_r	14.50P_r	Row 3	3.1I_r	5V_r	15.50P_r	
Row 3	2.8I_r	4V_r	11.20P_r	Row 5	2.5I_r	4V_r	10.00P_r	Row 1	3I_r	4V_r	12.00P_r	Row 4	3.1I_r	4V_r	12.40P_r	
Row 5	3.2I_r	3V_r	9.60P_r	Row 4	3.5I_r	3V_r	10.50P_r	Row 2	3.5I_r	3V_r	10.50P_r	Row 1	3.4I_r	3V_r	10.20P_r	
Row 1	4I_r	2V_r	8.00P_r	Row 2	4I_r	2V_R	8.00P_r	Row 3	3.5I_r	2V_r	7.00P_r	Row 2	3.4I_r	2V_r	6.80P_r	
Row 2	4I_r	V_r	4.00P_R	Row 3	4I_r	V_r	4.00P_R	Row 5	3.6I_r	V_r	4.00P_R	Row 5	3.5I_r	V_r	3.50P_r	

For the CS technique, the current output from all five rows ($I_{Row1(CS)}$ to $I_{Row5(CS)}$) of the array has been calculated as

$$I_{Row1(CS)} = I_{R2(CS)} = I_{R5(CS)} = 5^*(0.8)I_r = 4.0I_r \quad (30)$$

$$I_{Row3(CS)} = 2^*(0.1)I_r + 3^*(0.8)I_r = 2.6I_r \quad (31)$$

$$I_{Row3(CS)} = 3^*(0.2)I_r + 2^*(0.8)I_r = 2.2I_r \quad (32)$$

For the SD-PAR technique, the current output from all five rows ($I_{Row1(SD)}$ to $I_{Row5(SD)}$) of the array has been calculated as

$$I_{Row1(SD)} = I_{R5(SD)} = 0.1I_r + 0.2I_r + 3^*(0.8)I_r = 2.7I_r \quad (33)$$

$$I_{Row2(Fut)} = I_{Row3(Fut)} = 5^*(0.8)I_r = 4.0I_r \quad (34)$$

$$I_{Row4(SD)} = 4^*(0.8)I_r + 0.2I_r = 3.4I_r \quad (35)$$

For the OE technique, the current output from all the five rows ($I_{Row1(OE)}$ to $I_{Row5(OE)}$) of arrays has been calculated as

$$I_{Row1(OE)} = 0.1I_M + 4^*(0.8)I_r = 3.3I_r \quad (36)$$

$$I_{Row2(OE)} = I_{Row3(OE)} = 0.2I_r + 4^*(0.8)I_r = 3.4I_r \quad (37)$$

$$I_{Row4(OE)} = 0.1I_M + 0.2I_M + 3^*(0.8)I_M = 2.7I_r \quad (38)$$

$$I_{Row5(OE)} = 5^*(0.8)I_r = 4.0I_r \quad (39)$$

Similarly, for the HSR, the current output from five rows ($I_{Row1(HSR)}$ to $I_{Row5(HSR)}$) of the arrays has been calculated as

$$I_{Row1(HSR)} = I_{Row3(HSR)} = 0.1I_r + 4^*(0.8)I_r = 3.3I_r \quad (40)$$

TABLE 2. Theoretical calculation of current, voltage, and power of different techniques during cases A5 to A8.

Partial Shading A5																
TCT				**Sudoku**				**Futoshiki**				**MS**				
Row	***I***	***V***	***P***	***Row***	***I***	***V***	***P***	***Row***	***I***	***V***	***P***	***Row***	***I***	***V***	***P***	
Row 1	2.45I_r	5V_r	12.25P_r	Row 1	2.45I_r	5V_r	12.25P_r	Row 1	2.45I_r	5V_r	12.25P_r	Row 1	2.85I_r	5V_r	14.25P_r	
Row 2	2.45I_r	4V_r	9.80P_r	Row 2	2.85I_r	4V_r	11.40P_r	Row 4	2.85I_r	4V_r	11.40P_r	Row 2	3I_r	4V_r	12.00P_r	
Row 3	2.45I_r	3V_r	7.35P_r	Row 5	3.05 I_r	3V_r	9.15 P_r	Row 3	3I_r	3V_r	9.00P_r	Row 3	3I_r	3V_r	9.00P_r	
Row 4	4I_r	2V_r	8.00P_r	Row 3	3.4I_r	2V_r	6.80P_r	Row 5	3.45I_r	2V_r	6.90P_r	Row 4	3.05I_r	2V_r	6.10P_r	
Row 5	4I_R	V_r	4.00P_r	Row 5	3.6I_r	V_R	3.60P_r	Row 2	3.6I_r	V_r	3.60P_r	Row 5	3.45I_r	V_r	3.45P_r	
CS				**SD-PAR**				**OE**				**HSR**				
Row	***I***	***V***	***P***	***Row***	***I***	***V***	***P***	***Row***	***I***	***V***	***P***	***Row***	***I***	***V***	***P***	
Row 3	2.2I_r	5V_r	11.00P_r	Row 5	2.45I_r	5V_r	12.25P_r	Row 1	2I_r	5V_r	10.00P_r	Row 3	3.0I_r	5V_r	15.00P_r	
Row 4	2.35I_r	4V_r	9.40P_r	Row 1	2.85I_r	4V_r	11.40P_r	Row 4	2.85I_r	4V_r	11.40P_R	Row 1	3.05I_r	4V_r	12.20P_r	
Row 5	2.8I_r	3V_r	8.40P_r	Row 4	3.05I_r	3V_r	12.20P_r	Row 2	3.45I_r	3V_r	10.35P_r	Row 2	3.15I_r	3V_r	9.45P_r	
Row 1	4I_r	2V_r	8.00P_r	Row 2	3.4I_r	2V_r	6.80P_r	Row 3	3.45I_r	2V_r	6.90P_r	Row 5	3.15I_r	2V_r	6.30P_r	
Row 2	4I_r	V_r	4.00P_r	Row 3	3.6I_r	V_r	3.60P_r	Row 5	3.6I_r	V_r	3.60P_r	Row 4	3.45I_r	V_r	3.45P_r	
Partial Shading A6																
TCT				**Sudoku**				**Futoshiki**				**MS**				
Row	***I***	***V***	***P***	***Row***	***I***	***V***	***P***	***Row***	***I***	***V***	***P***	***Row***	***I***	***V***	***P***	
Row 1	2.6I_r	5V_r	13.00P_r	Row 1	2.8I_r	5V_r	14.00P_r	Row 1	2.8I_r	5V_r	14.00P_r	Row 4	2.8I_r	5V_r	14.00P_r	
Row 2	2.8I_r	4V_r	11.20P_r	Row 2	3.1I_r	4V_r	12.40P_r	Row 4	2.9I_r	4V_r	11.60P_r	Row 1	3.1I_r	4V_r	12.40P_r	
Row 3	2.8I_r	3V_r	8.40P_r	Row 4	3.2I_r	3V_r	9.60P_r	Row 2	3.2I_r	3V_r	9.60P_r	Row 2	3.2I_r	3V_r	9.60P_r	
Row 4	3.5I_r	2V_r	7.00P_r	Row 3	3.3I_r	2V_r	6.60P_r	Row 3	3.2I_r	2V_R	6.40P_r	Row 3	3.2I_r	2V_r	6.40P_r	
Row 5	4I_r	V_r	4.00P_R	Row 5	3.3I_r	V_r	3.30P_R	Row 5	3.6I_r	V_R	3.60P_R	Row 5	3.4I_r	V_r	3.40P_R	
CS				**SD-PAR**				**OE**				**HSR**				
Row	***I***	***V***	***P***	***Row***	***I***	***V***	***P***	***Row***	***I***	***V***	***P***	***Row***	***I***	***V***	***P***	
Row 3	2I_r	5V_r	10.00P_r	Row 5	2.8I_r	5V_r	14.00P_r	Row 1	2.4I_r	5V_r	12.00P_r	Row 1	3.1I_r	5V_r	15.50P_r	
Row 4	2.8I_r	4V_r	11.20P_r	Row 1	3.1I_r	4V_r	12.40P_r	Row 2	3.6I_r	4V_r	14.40P_r	Row 2	3.1I_r	4V_r	12.40P_r	
Row 5	3.1I_r	3V_r	9.30P_r	Row 3	3.2I_r	3V_r	9.60P_r	Row 3	3.4I_r	3V_r	10.20P_r	Row 5	3.1I_r	3V_r	9.30P_r	
Row 1	3.8I_r	2V_r	7.60P_r	Row 2	3.3I_r	2V_r	6.60P_r	Row 4	3.1I_r	2V_r	6.20P_r	Row 3	3.2I_r	2V_R	6.40P_r	
Row 2	4I_r	V_R	4.00P_r	Row 5	3.3I_r	V_r	3.30P_r	Row 5	3.2I_r	V_r	3.20P_R	Row 4	3.2I_R	V_r	3.20P_r	
Partial Shading A7																
TCT				**Sudoku**				**Futoshiki**				**MS**				
Row	***I***	***V***	***P***	***Row***	***I***	***V***	***P***	***Row***	***I***	***V***	***P***	***Row***	***I***	***V***	***P***	
Row 2	2.95I_r	5V_r	14.75P_r	Row 1	3.15I_r	5V_M	15.75P_r	Row 1	3.1I_r	5V_r	15.50P_r	Row 1	3.25I_r	5V_r	16.25P_r	
Row 3	3I_r	4V_r	11.80P_r	Row 2	3.6I_R	4V_M	14.40P_r	Row 2	3.25I_r	4V_r	13.00P_r	Row 2	3.45I_R	4V_r	13.80P_r	
Row 4	3.25I_r	3V_r	9.00P_r	Row 3	3.5I_r	3V_M	10.50P_r	Row 3	3.6I_r	3V_r	10.80P_r	Row 3	3.5I_r	3V_r	10.50P_r	
Row 5	3.85I_r	2V_r	6.50P_r	Row 4	3.25I_r	2V_M	6.50P_r	Row 4	3.85I_r	2V_r	7.70P_r	Row 4	3.25I_r	2V_r	6.50P_r	
Row 1	4I_r	V_r	4P_r	Row 5	3.25I_r	V_M	3.25P_r	Row 5	3.25I_r	V_r	3.25P_r	Row 5	3.6I_r	V_r	3.60P_r	
CS				**SD-PAR**				**OE**				**HSR**				
Row	***I***	***V***	***P***	***Row***	***I***	***V***	***P***	***Row***	***I***	***V***	***P***	***Row***	***I***	***V***	***P***	
Row 2	3.1I_r	5V_r	15.50P_r	Row 3	3.25I_r	5V_r	16.25P_r	Row 5	2.85I_r	5V_r	11.40P_r	Row 2	3.4I_r	5V_r	17.00P_r	
Row 1	3.25I_r	4V_r	13.00P_r	Row 4	3.25I_r	4V_r	13.00P_r	Row 3	3.35I_r	4V_r	13.40P_r	Row 3	3.4I_r	4V_r	13.60P_r	
Row 5	3.25I_r	3V_r	9.75P_r	Row 5	3.45I_r	3V_r	10.35P_r	Row 4	3.5I_r	3V_r	10.50P_r	Row 4	3.4I_r	3V_r	10.20P_r	
Row 4	3.6I_r	2V_r	7.20P_r	Row 2	3.5I_r	2V_r	7.00P_r	Row 2	3.6I_r	2V_r	7.20P_r	Row 5	3.4I_r	2V_r	6.80P_r	
Row 3	3.85I_r	V_r	3.85P_r	Row 1	3.6I_r	V_r	3.60P_r	Row 1	3.75I_r	V_r	3.75P_r	Row 1	3.45I_r	V_r	3.45P_r	
Partial Shading A8																
TCT				**Sudoku**				**Futoshiki**				**MS**				
Row	***I***	***V***	***P***	***Row***	***I***	***V***	***P***	***Row***	***I***	***V***	***P***	***Row***	***I***	***V***	***P***	
Row 3	3.1I_r	5V_r	15.50P_r	Row 3	3.1I_r	5V_r	15.50P_r	Row 5	3I_r	5V_r	15.00P_r	Row 5	2.95I_r	5V_r	14.75P_r	
Row 1	3.2I_r	4V_r	12.80P_r	Row 4	3.2I_r	4V_r	12.80P_r	Row 3	3.15I_r	4V_r	12.60P_r	Row 4	3.2I_r	4V_r	12.80P_r	
Row 5	3.25I_r	3V_r	9.75P_r	Row 2	3.25I_r	3V_r	9.75P_r	Row 2	3.2I_r	3V_r	9.60P_r	Row 3	3.25I_r	3V_r	9.75P_r	
Row 2	3.3I_r	2V_r	6.60P_r	Row 1	3.35I_r	2V_r	6.70P_r	Row 4	3.25I_r	2V_r	6.50P_r	Row 1	3.3I_r	2V_r	6.60P_r	
Row 4	3.4I_r	V_r	3.40P_r	Row 5	3.35I_r	V_r	3.35P_r	Row 1	3.65I_r	V_R	3.65P_R	Row 2	3.55I_r	V_r	3.55P_r	
CS				**SD-PAR**				**OE**				**HSR**				
Row	***I***	***V***	***P***	***Row***	***I***	***V***	***P***	***Row***	***I***	***V***	***P***	***Row***	***I***	***V***	***P***	
Row 1	2.61 I_r	5V_r	13.00P_r	Row 2	3.1I_r	5V_r	15.50P_r	Row 3	3.05I_r	5V_r	15.25P_r	Row 1	3.25I_r	5V_r	16.25P_r	
Row 2	2.61 I_r	4V_r	10.40P_r	Row 3	3.2I_r	4V_r	12.80P_r	Row 2	3.25I_r	4V_r	13.00P_r	Row 2	3.25I_r	4V_r	13.00P_r	
Row 5	3.35I_r	3V_r	10.05P_r	Row 1	3.25I_r	3V_r	9.75P_r	Row 5	3.25I_r	3V_r	9.75P_r	Row 3	3.25I_r	3V_r	9.75P_r	
Row 3	3.85I_r	2V_r	7.70P_r	Row 4	3.35I_r	2V_r	6.70P_r	Row 1	3.3I_r	2V_R	6.60P_r	Row 4	3.25I_r	2V_r	6.50P_r	
Row 4	3.85I_r	V_r	3.85P_r	Row 5	3.35I_r	V_r	3.35P_r	Row 4	3.4I_r	V_r	3.40P_r	Row 5	3.25I_r	V_r	3.25P_r	

$$I_{Row2(HSR)} = I_{Row4(HSR)} = I_{Row5(HSR)} = 0.2I_r + 4^*(0.8)I_r = 3.4I_r \quad (41)$$

It can be noticed from the above mathematical calculations that each technique exhibits a notable different between the row current values however, in the HSR, the differences get reduced with all the rows generating nearly equal currents. The theoretical power calculation from different techniques during case A3 has been done in TABLE 1 in which it can be seen that TCT, Sudoku, Futoshiki, MS, SD-PAR, and OE have equal theoretical power of $13.50P_r$ whereas CS has the lowest value of $12P_r$. The HSR has higher power of $16.50P_r$ which proves the efficient shade dispersion capability during shading. The P-V curves (FIGURE 7 (c)) show higher power output in HSR (5.72kW) than SP (4.59kW), TCT (4.85kW), Sudoku (4.85kW), Futoshiki (4.91 kW), MS (4.92kW), CS (4.11kW), SD-PAR (4.84kW) and OE (4.93kW).

4) CASE A4 (28% SHADING)

The shading case shown in FIGURE 5 (d) and dispersion of shade shown in FIGURE 6 (b) reflect multiple irradiances of 200W/m^2, 300W/m^2, and 400W/m^2 in 1st, 2nd and 3rd columns of the PV array. The theoretical calculation given in TABLE 1 shows the efficient dispersion

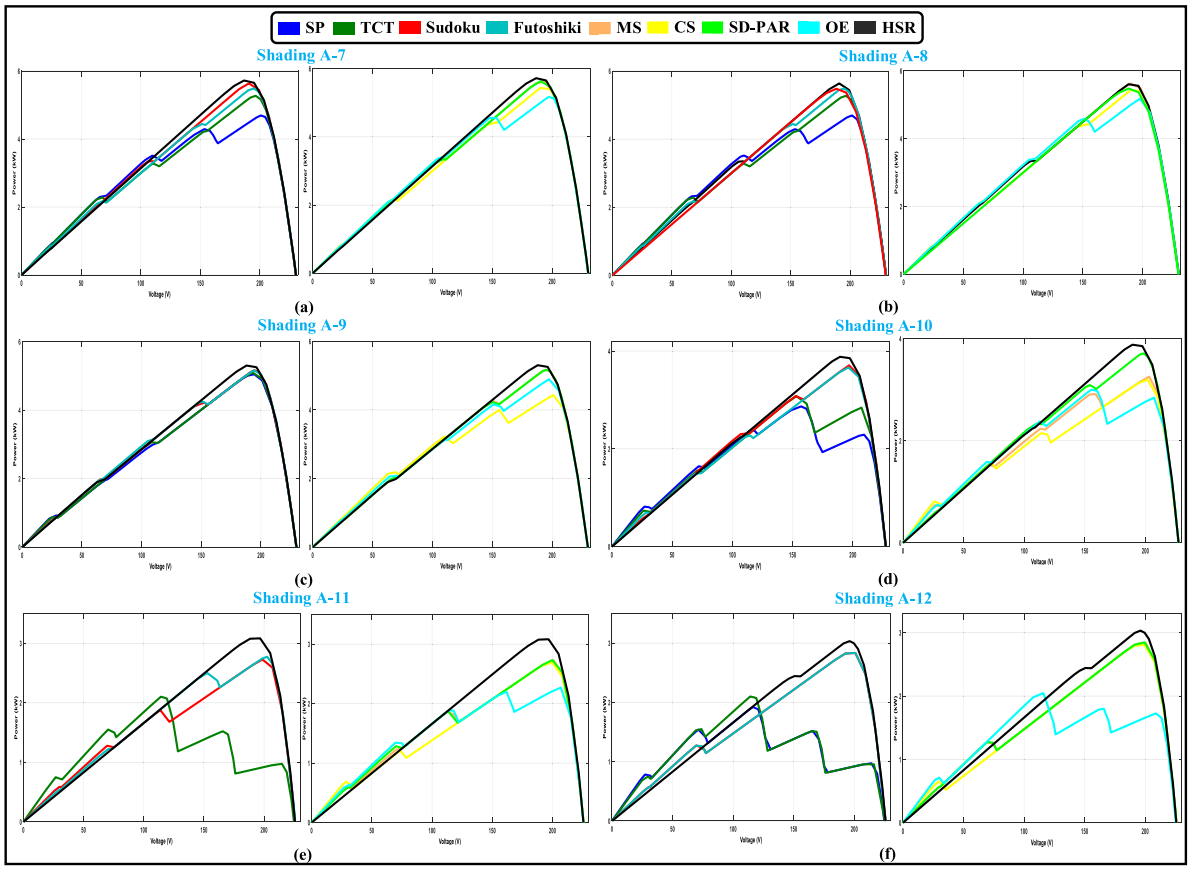

FIGURE 8. P-V curves of different PV array configuration techniques during shading cases (a) A7, (b) A8, (c) A9, (d) A10, (e) A11, and (f) A12.

with a maximized power output of $15.50P_r$ in the proposed HSR as compared to TCT, Futoshiki, MS, and OE with $14.50P_r$ and Sudoku, CS, and SD-PAR with $12.50P_r$. The P-V curves shown in FIGURE 7 (d), HSR has convex curve with maximum power output of 5.51kW as compared to SP (4.32kW), TCT (4.59kW), Sudoku (4.60kW), Futoshiki (4.61kW), MS (5.20kW), CS (4.59kW), SD-PAR (4.60kW) and OE (5.17kW) with peaks count higher than one in the curves.

5) CASE A5 (36% SHADING)

During case A5 (FIGURE 5(e)), HSR has generated higher theoretical power output of $15P_r$ than the TCT ($12.25P_r$), Sudoku ($12.25P_r$), Futoshiki ($12.25P_r$), MS ($14.25P_r$), CS ($11P_r$), SD-PAR ($12.25P_r$) and OE ($11.40P_r$) [from shade dispersion in FIGURE 6 (c) and calculation in TABLE 2]. The P-V curves in FIGURE 7 (e) show that HSR has higher power output of 5.32kW and generated convex curve as compared to the SP (4.47kW), TCT (4.61kW), Sudoku (4.73 kW), Futoshiki (4.73kW), MS (5.20 kW), CS (4.33kW), SD-PAR (4.74kW) and OE (4.21kW). The enhancement in power by TCT, Sudoku, Futoshiki, MS, CS, SD-PAR, OE, and HSR than the SP are noted as 3.13%, 5.82%, 5.82%, 16.33%, -3.13%, 6.04%, -5.82% and 19.02% respectively.

6) CASE A6 (44% SHADING)

The shading case A6, theoretical power outputs calculations, and P-V curves of different techniques have been given in FIGURE 5 (f), TABLE 2, and FIGURE 7 (f) respectively. The HSR has shown higher performance with $15.50P_r$ and 5.36kW as theoretical and actual power outputs as compared to the SP (4.55kW), TCT ($13P_r$, 4.70kW), Sudoku ($14P_r$, 5.02kW), Futoshiki ($14P_r$, 4.99kW), MS ($14P_r$, 5.01kW), CS ($11.20\ P_r$, 3.99kW), SD-PAR ($14P_r$, 5.02kW) and OE ($14.40P_r$, 4.44kW). The proposed HSR has 17.80% higher power output than the SP whereas TCT, Sudoku, Futoshiki, MS, CS, SD-PAR, and OE have enhancement of 3.30%, 10.33%, 9.67%, 10.11%, -12.31%, 10.33% and -2.42% than SP respectively.

7) CASE A7 (52% SHADING)

During this case (FIGURE 5 (g)), the maximum theoretical power generations of the HSR has been calculated as $17P_r$ which is higher than the TCT ($14.75P_r$), Sudoku ($15.75P_r$), Futoshiki ($15.50P_r$), MS ($16.25P_r$), CS ($15.50P_r$, SD-PAR ($16.25P_r$) and OE ($11.40P_r$). The P-V curves of different array techniques during this shading case have been depicted in FIGURE 8 (a) where it is noticed that all the techniques have exhibited multiple peaks which is not in the case of HSR (convex curve). The maximum powers have

TABLE 3. Theoretical calculation of current, voltage, and power of different techniques during cases A9 to A12.

Partial Shading A-9																
TCT				**Sudoku**				**Futoshiki**				**MS**				
Row	I	V	P	Row	I	V	P	Row	I	V	P	Row	I	V	P	
Row 3	$2.9I_r$	$5V_r$	$14.50P_r$	Row 4	$2.9I_r$	$5V_r$	$14.50P_r$	Row 2	$2.9I_r$	$5V_r$	$14.50P_r$	Row 3	$2.9I_r$	$5V_r$	$14.40P_r$	
Row 4	$2.9I_r$	$4V_r$	$11.60P_r$	Row 3	$3.1I_r$	$4V_r$	$12.40P_r$	Row 5	$3.1I_r$	$4V_r$	$12.40P_r$	Row 5	$3.1I_r$	$4V_r$	$12.40P_r$	
Row 1	$3.1I_r$	$3V_r$	$9.30P_r$	Row 5	$3.1I_r$	$3V_r$	$9.30P_r$	Row 4	$3.2I_r$	$3V_r$	$9.60P_r$	Row 1	$3.2I_r$	$3V_r$	$9.60P_r$	
Row 2	$3.1I_r$	$2V_r$	$6.20P_r$	Row 2	$3.3I_r$	$2V_r$	$6.60P_r$	Row 3	$3.3I_r$	$2V_r$	$6.60P_r$	Row 4	$3.3I_r$	$2V_r$	$6.60P_r$	
Row 5	$3.9I_r$	V_r	$3.90P_r$	Row 1	$3.5I_r$	V_r	$3.50P_R$	Row 1	$3.4I_r$	V_r	$3.40P_r$	Row 2	$3.4I_r$	V_r	$3.40P_R$	
CS				**SD-PAR**				**OE**				**HSR**				
Row	I	V	P	Row	I	V	P	Row	I	V	P	Row	I	V	P	
Row 2	$2.4I_r$	$5V_r$	$12.00P_r$	Row 3	$2.9I_r$	$5V_r$	$14.50P_r$	Row 5	$2.7I\ I_r$	$5V_r$	$13.50P_r$	Row 1	$3.1I_r$	$5V_r$	$15.50P_r$	
Row 1	$2.8I_r$	$4V_r$	$11.20P_r$	Row 2	$3.1I_r$	$4V_r$	$12.40P_r$	Row 3	$3.0I\ I_r$	$4V_r$	$12.00P_r$	Row 2	$3.1I_r$	$4V_r$	$12.40P_r$	
Row 5	$3.2I_r$	$3V_r$	$9.60P_r$	Row 4	$3.1I_r$	$3V_r$	$9.30P_r$	Row 1	$3.1I\ I_r$	$3V_r$	$9.30P_r$	Row 3	$3.1I_r$	$3V_r$	$9.30P_r$	
Row 4	$3.7I_r$	$2V_r$	$7.40P_r$	Row 1	$3.3I_r$	$2V_r$	$6.60P_r$	Row 4	$3.5I\ I_r$	$2V_r$	$7.00P_r$	Row 4	$3.3I_r$	$2V_r$	$6.60P_r$	
Row 3	$3.8I_r$	V_r	$3.80P_r$	Row 5	$3.5I_r$	V_r	$3.50P_r$	Row 2	$3.6I\ I_r$	V_r	$3.60P_r$	Row 5	$3.3I_r$	V_r	$3.30P_r$	
Partial Shading A-10																
TCT				**Sudoku**				**Futoshiki**				**MS**				
Row	I	V	P	Row	I	V	P	Row	I	V	P	Row	I	V	P	
Row 4	$1.5I_r$	$5V_r$	$7.50P_r$	Row 2	$2.1I_r$	$5V_r$	$10.50P_r$	Row 3	$2.1I_r$	$5V_r$	$10.50P_r$	Row 1	$1.8I_r$	$5V_r$	$9.00P_r$	
Row 3	$2.2I_r$	$4V_r$	$8.80P_r$	Row 4	$2.25I_r$	$4V_r$	$9.00P_r$	Row 4	$2.1I_r$	$4V_r$	$8.40P_r$	Row 3	$2.1I_r$	$4V_r$	$8.40P_r$	
Row 5	$2.35I_r$	$3V_r$	$7.05P_r$	Row 1	$2.35I_r$	$3V_r$	$7.05P_r$	Row 2	$2.25I_r$	$3V_r$	$6.75P_r$	Row 4	$2.2I_r$	$3V_r$	$6.60P_r$	
Row 2	$2.4I_r$	$2V_r$	$4.80P_r$	Row 5	$2.35I_r$	$2V_r$	$4.70P_r$	Row 1	$2.35I_r$	$2V_r$	$4.70P_r$	Row 2	$2.35I_r$	$2V_r$	$4.70P_r$	
Row 1	$3.1I_r$	V_r	$3.10P_r$	Row 3	$2.5I_r$	V_r	$2.50P_r$	Row 5	$2.75I_R$	V_r	$2.75P_r$	Row 5	$3.1I_r$	V_r	$3.10P_r$	
CS				**SD-PAR**				**OE**				**HSR**				
Row	I	V	P	Row	I	V	P	Row	I	V	P	Row	I	V	P	
Row 4	$1.8I_r$	$5V_r$	$9.00P_r$	Row 1	$2.1I_r$	$5V_r$	$10.50P_r$	Row 4	$1.6I_r$	$5V_r$	$8.00P_r$	Row 4	$2.25I_r$	$5V_r$	$11.25P_r$	
Row 5	$1.8I_r$	$4V_r$	$7.20P_r$	Row 3	$2.25I_r$	$4V_R$	$9.00P_r$	Row 5	$2.1I_r$	$4V_r$	$8.40P_r$	Row 5	$2.25I_r$	$4V_r$	$9.00P_r$	
Row 1	$2.1I_r$	$3V_r$	$6.30P_R$	Row 5	$2.25I_R$	$3V_r$	$6.75P_r$	Row 3	$2.30I_r$	$3V_r$	$6.90P_r$	Row 1	$2.3I_r$	$3V_r$	$6.90P_r$	
Row 3	$2.35I_r$	$2V_r$	$4.70P_r$	Row 4	$2.35I_r$	$2V_r$	$4.70P_r$	Row 1	$2.5I_r$	$2V_r$	$5.00P_r$	Row 2	$2.3I_r$	$2V_r$	$4.60P_r$	
Row 2	$3.5I_r$	V_r	$3.50P_r$	Row 2	$2.5I_r$	V_r	$2.50P_r$	Row 2	$3.05I_r$	V_R	$3.05P_r$	Row 3	$2.3I_r$	V_r	$2.30P_r$	
Partial Shading A-11																
TCT				**Sudoku**				**Futoshiki**				**MS**				
Row	I	V	P	Row	I	V	P	Row	I	V	P	Row	I	V	P	
Row 5	$0.50I_r$	$5V_r$	$2.50P_r$	Row 1	$1.5I_r$	$5V_r$	$7.50P_r$	Row 1	$1.5I_r$	$5V_r$	$7.50P_r$	Row 1	$1.5I_r$	$5V_r$	$7.50P_r$	
Row 4	$1I_r$	$4V_r$	$4.00P_r$	Row 5	$1.5I_r$	$4V_r$	$6.00P_r$	Row 3	$1.8I_r$	$4V_r$	$6.00P_r$	Row 2	$1.5I_r$	$4V_r$	$6.00P_r$	
Row 3	$2I_r$	$3V_r$	$6.00P_r$	Row 2	$1.8I_r$	$3V_r$	$5.40P_r$	Row 4	$1.8I_r$	$3V_r$	$5.40P_r$	Row 3	$1.8I_r$	$3V_r$	$5.40P_r$	
Row 2	$2.4I_r$	$2V_r$	$4.80P_r$	Row 4	$2I_r$	$2V_r$	$4.00P_r$	Row 5	$1.9I_r$	$2V_r$	$3.80P_r$	Row 4	$1.9I_r$	$2V_r$	$3.80P_r$	
Row 1	$3.1I_r$	V_r	$3.10P_r$	Row 3	$2.2I_r$	V_r	$2.20P_R$	Row 2	$2I_r$	V_R	$2.00P_r$	Row 5	$2.3I_r$	V_r	$2.30P_R$	
CS				**SD-PAR**				**OE**				**HSR**				
Row	I	V	P	Row	I	V	P	Row	I	V	P	Row	I	V	P	
Row 3	$1.5I_r$	$5V_r$	$7.50P_r$	Row 5	$1.4I_r$	$5V_r$	$7.00P_r$	Row 4	$1.2I_r$	$5V_r$	$6.00P_r$	Row 1	$1.8I_r$	$5V_r$	$9.00P_r$	
Row 4	$1.5I_r$	$4V_r$	$6.00P_r$	Row 4	$1.5I_r$	$4V_r$	$6.00P_r$	Row 2	$1.5I_r$	$4V_r$	$6.00P_r$	Row 2	$1.8I_r$	$4V_r$	$7.20P_r$	
Row 5	$1.5I_r$	$3V_r$	$4.50P_r$	Row 1	$1.8I_r$	$3V_r$	$5.40P_r$	Row 5	$1.8I_r$	$3V_r$	$5.40P_r$	Row 3	$1.8I_r$	$3V_r$	$5.40P_r$	
Row 1	$1.8I_r$	$2V_r$	$3.60P_r$	Row 3	$2I_r$	$2V_r$	$4.00P_R$	Row 3	$2.1I_r$	$2V_r$	$4.20P_r$	Row 4	$1.8I_r$	$2V_r$	$3.60P_r$	
Row 2	$2.7I_R$	V_R	$2.70P_r$	Row 2	$2.2I_r$	V_r	$2.20P_R$	Row 1	$2.4I_r$	V_r	$2.40P_r$	Row 5	$1.8I_r$	V_r	$1.80P_r$	
Partial Shading A-12																
TCT				**Sudoku**				**Futoshiki**				**MS**				
Row	I	V	P	Row	I	V	P	Row	I	V	P	Row	I	V	P	
Row 1	$0.5I_r$	$5V_r$	$2.50P_r$	Row 1	$1.6I_r$	$5V_r$	$8.00P_r$	Row 1	$1.6I_r$	$5V_r$	$8.00P_r$	Row 2	$1.6I_r$	$5V_r$	$8.00P_r$	
Row 2	$1I_r$	$4V_r$	$4.00P_r$	Row 2	$1.6I_r$	$4V_r$	$6.40P_r$	Row 3	$1.6I_r$	$4V_r$	$6.40P_r$	Row 3	$1.6I_r$	$4V_r$	$6.40P_r$	
Row 3	$2I_r$	$3V_r$	$6.00P_r$	Row 3	$1.6I_r$	$3V_r$	$4.80P_r$	Row 5	$1.6I_r$	$3V_r$	$4.80P_r$	Row 4	$1.6I_r$	$3V_r$	$4.80P_r$	
Row 4	$2.4I_r$	$2V_r$	$4.80P_r$	Row 5	$2I_r$	$2V_r$	$4.00P_r$	Row 4	$2I_r$	$2V_r$	$4.00P_r$	Row 1	$2I_R$	$2V_r$	$4.00P_r$	
Row 5	$3I_r$	V_r	$3.00P_r$	Row 4	$2.1I_r$	V_r	$2.10P_r$	Row 2	$2.1I_r$	V_r	$2.10P_r$	Row 5	$2.1I_r$	V_r	$2.10P_r$	
CS				**SD-PAR**				**OE**				**HSR**				
Row	I	V	P	Row	I	V	P	Row	I	V	P	Row	I	V	P	
Row 1	$1.6I_r$	$5V_r$	$8.00P_r$	Row 1	$1.6I_r$	$5V_r$	$8.00P_r$	Row 1	$0.9I_r$	$5V_r$	$4.50P_r$	Row 3	$1.7I_r$	$5V_r$	$8.50P_r$	
Row 3	$1.6I_r$	$4V_r$	$6.40P_r$	Row 2	$1.6I_r$	$4V_r$	$6.40P_r$	Row 3	$1.2I_r$	$4V_r$	$4.80P_r$	Row 1	$1.8I_r$	$4V_r$	$7.20P_r$	
Row 4	$1.6I_r$	$3V_r$	$4.80P_r$	Row 5	$1.7I_r$	$3V_r$	$5.10P_r$	Row 4	$2I_r$	$3V_r$	$6.00P_r$	Row 2	$1.8I_r$	$3V_r$	$5.40P_r$	
Row 5	$1.6I_r$	$2V_r$	$3.20P_r$	Row 4	$2I_r$	$2V_r$	$4.00P_r$	Row 5	$2I_r$	$2V_r$	$4.00P_r$	Row 4	$1.8I_r$	$2V_r$	$3.60P_r$	
Row 2	$2.5I_R$	V_r	$2.10P_r$	Row 3	$2.1Ir_M$	V_r	$2.10P_r$	Row 2	$2.8I_r$	V_r	$2.80P_r$	Row 5	$1.8I_r$	V_r	$1.80P_r$	

been noted as 4.69kW, 5.27kW, 5.63kW, 5.48kW, 5.61kW, 5.43kW, 5.63 kW, 5.17kW by SP, TCT, Sudoku, Futoshiki, MS, CS, SD-PAR, and OE respectively which is lower than the proposed HSR technique i.e., 5.92kW.

8) CASE A8 (60% SHADING)

The shading case has been shown in FIGURE 5 (h) whereas FIGURE 8 (b) shows the P-V curves by different techniques in which it can be observed that the HSR generated comparatively higher power output (5.97kW) than the SP (4.69kW), TCT (5.27kW), Sudoku (5.63kW), Futoshiki (5.48 kW), MS (5.62kW), CS (5.43kW), SD-PAR (5.60kW) and OE (5.17kW). TABLE 2 shows the theoretical power output of different techniques in which it has been found that HSR has higher value of $16.25P_r$ than others. The available power deviation of SP, TCT, Sudoku, Futoshiki, MS, CS, SD-PAR, OE, and HSR have been calculated as -16.70%, -6.39%, -6%, -2.66%, -2.18%, -3.55%, -2.53%, -8.17% and -1.07%.

9) CASE A9 (68% SHADING)

During this shading case (FIGURE 5 (i)), HSR generated a higher power output of 5.40kW and $15.50P_r$ (theoretical power established from TABLE 3). The CS has the lowest power output of 4.43kW and $12P_r$ followed by OE (4.89kW and $13.50P_r$), SP (5.04kW), TCT (5.09kW and $14.50P_r$), Sudoku and Futoshiki (5.16kW and $14.50P_r$),

TABLE 4. Summarized results of different 5 × 5 PV array techniques during shading cases A1 to A12.

Power Output (in kW)												
Technique	**A-1**	**A-2**	**A-3**	**A-4**	**A-5**	**A-6**	**A-7**	**A-8**	**A-9**	**A-10**	**A-11**	**A-12**
SP	5.56	4.6	4.59	4.32	4.47	4.55	4.69	4.69	5.04	2.86	2.01	1.92
TCT	5.56	4.81	4.85	4.59	4.61	4.7	5.27	5.27	5.09	3.07	2.1	2.1
Sudoku	5.56	5.71	4.85	4.6	4.73	5.02	5.63	5.63	5.16	3.7	2.72	2.83
Futoshiki	5.56	5.71	4.91	4.61	4.73	4.99	5.48	5.48	5.16	3.66	2.77	2.84
MS	5.56	5.71	4.92	5.2	5.2	5.01	5.61	5.62	5.17	3.25	2.73	2.83
CS	5.56	4.81	4.11	4.59	4.33	3.99	5.43	5.43	4.43	3.19	2.69	2.8
SD-PAR	5.56	5.71	4.84	4.6	4.74	5.02	5.63	5.6	5.17	3.71	2.73	2.84
OE	5.56	5.71	4.93	5.17	4.21	4.44	5.17	5.17	4.89	2.99	2.27	2.04
HSR	5.56	5.71	5.72	5.51	5.32	5.36	5.92	5.97	5.40	3.98	3.18	3.23
Power Loss (in %)												
Technique	**A-1**	**A-2**	**A-3**	**A-4**	**A-5**	**A-6**	**A-7**	**A-8**	**A-9**	**A-10**	**A-11**	**A-12**
SP	16.01	30.51	30.66	34.74	32.48	31.27	29.15	29.15	23.87	56.80	69.64	71.00
TCT	16.01	27.34	26.74	30.66	30.36	29.00	20.39	20.39	23.11	53.63	68.28	68.28
Sudoku	16.01	13.75	26.74	30.51	28.55	24.17	14.95	16.95	22.05	44.11	58.91	57.25
Futoshiki	16.01	13.75	25.83	30.36	28.55	24.62	17.22	17.22	22.05	44.71	58.16	57.10
MS	16.01	13.75	25.68	21.45	21.45	24.32	15.26	16.11	21.90	50.91	58.76	57.25
CS	16.01	27.34	37.92	30.66	34.59	39.73	17.98	17.98	33.08	51.81	59.37	57.70
SD-PAR	16.01	13.75	26.89	30.51	28.40	24.17	14.95	15.41	21.90	43.96	58.76	57.10
OE	16.01	13.75	25.53	21.90	36.40	32.93	21.90	21.90	26.13	54.83	65.71	69.18
HSR	16.01	13.75	13.60	16.77	19.64	19.03	10.57	15.86	18.43	39.88	51.96	51.21
Power Enhancement than SP (in %)												
Technique	**A-1**	**A-2**	**A-3**	**A-4**	**A-5**	**A-6**	**A-7**	**A-8**	**A-9**	**A-10**	**A-11**	**A-12**
TCT	0	4.57	5.66	6.25	3.13	3.30	12.37	12.37	0.99	7.34	4.48	9.38
Sudoku	0	24.13	5.66	6.48	5.82	10.33	20.04	20.04	2.38	29.37	35.32	47.40
Futoshiki	0	24.13	6.97	6.71	5.82	9.67	16.84	14.84	2.38	27.97	37.81	47.92
MS	0	24.13	7.19	20.37	16.33	10.11	19.62	19.83	2.58	13.64	35.82	47.40
CS	0	4.57	-10.46	6.25	-3.13	-12.31	15.78	14.78	-12.10	11.54	33.83	45.83
SD-PAR	0	24.13	5.45	6.48	6.04	10.33	20.04	15.40	2.58	29.72	35.82	47.92
OE	0	24.13	7.41	19.68	-5.82	-2.42	10.23	10.23	-2.98	4.55	12.94	6.25
HSR	0	24.13	24.62	27.55	19.02	17.80	26.23	18.76	7.14	39.16	58.21	68.23
Available Power Deviation (in %)												
Technique	**A-1**	**A-2**	**A-3**	**A-4**	**A-5**	**A-6**	**A-7**	**A-8**	**A-9**	**A-10**	**A-11**	**A-12**
SP	-0.89	-20.14	-20.45	-22.44	-17.07	-16.21	-21.70	-16.70	-8.20	-29.21	-37.19	-41.10
TCT	-0.89	-16.49	-15.94	-17.59	-14.47	-13.44	-12.02	-6.39	-7.29	-24.01	-34.38	-35.58
Sudoku	-0.89	-0.87	-15.94	-17.41	-12.24	-7.55	-6.01	-6.00	-6.01	-8.42	-15.00	-13.19
Futoshiki	-0.89	-0.87	-14.90	-17.24	-12.24	-8.10	-8.51	-2.66	-6.01	-9.41	-13.44	-12.88
MS	-0.89	-0.87	-14.73	-6.64	-3.53	-7.73	-6.34	-2.18	-5.83	-19.55	-14.69	-13.19
CS	-0.89	-16.49	-28.77	-17.59	-19.67	-26.52	-9.35	-3.55	-19.31	-21.04	-15.94	-14.11
SD-PAR	-0.89	-0.87	-16.12	-17.41	-12.06	-7.55	-6.01	-2.53	-5.83	-8.17	-14.69	-12.88
OE	-0.89	-0.87	-14.56	-7.18	-21.89	-18.23	-13.69	-8.17	-10.93	-25.99	-29.06	-37.42
HSR	-0.89	-0.87	-0.87	-1.08	-1.30	-1.29	-1.17	-1.07	-1.64	-1.49	-0.63	-0.92
Efficiency (in %)												
Technique	**A-1**	**A-2**	**A-3**	**A-4**	**A-5**	**A-6**	**A-7**	**A-8**	**A-9**	**A-10**	**A-11**	**A-12**
SP	16.45	13.61	13.58	12.78	13.22	13.46	13.88	13.88	14.91	8.46	5.95	5.68
TCT	16.45	14.23	14.35	13.58	13.64	13.91	15.59	15.59	15.06	9.08	6.21	6.21
Sudoku	16.45	16.89	14.35	13.61	13.99	14.85	16.66	15.66	15.27	10.95	8.05	8.37
Futoshiki	16.45	16.89	14.53	13.64	13.99	14.76	16.21	16.21	15.27	10.83	8.20	8.40
MS	16.45	16.89	14.56	15.38	15.38	14.82	16.60	15.63	15.30	9.62	8.08	8.37
CS	16.45	14.23	12.16	13.58	12.81	11.80	16.07	16.07	13.11	9.44	7.96	8.28
SD-PAR	16.45	16.89	14.32	13.61	14.02	14.85	16.66	16.57	15.30	10.98	8.08	8.40
OE	16.45	16.89	14.59	15.30	12.46	13.14	15.30	15.30	14.47	8.85	6.72	6.04
HSR	16.45	16.89	16.92	16.30	15.74	15.86	17.51	16.48	15.98	11.78	9.41	9.56
Peaks in Power Curves												
Technique	**A-1**	**A-2**	**A-3**	**A-4**	**A-5**	**A-6**	**A-7**	**A-8**	**A-9**	**A-10**	**A-11**	**A-12**
SP	2	3	3	4	2	4	4	4	2	5	5	5
TCT	2	3	3	4	2	4	4	3	3	4	4	5
Sudoku	2	2	3	4	4	4	2	3	3	3	4	2
Futoshiki	2	2	3	4	3	4	3	2	3	4	4	2
MS	2	2	3	3	2	2	2	2	3	5	4	2
CS	2	3	3	4	4	4	3	3	4	4	3	2
SD-PAR	2	2	3	4	4	3	2	2	3	3	4	2
OE	2	2	3	3	3	4	3	3	4	5	5	4
HSR	2	2	1	1	1	1	1	1	1	1	1	2

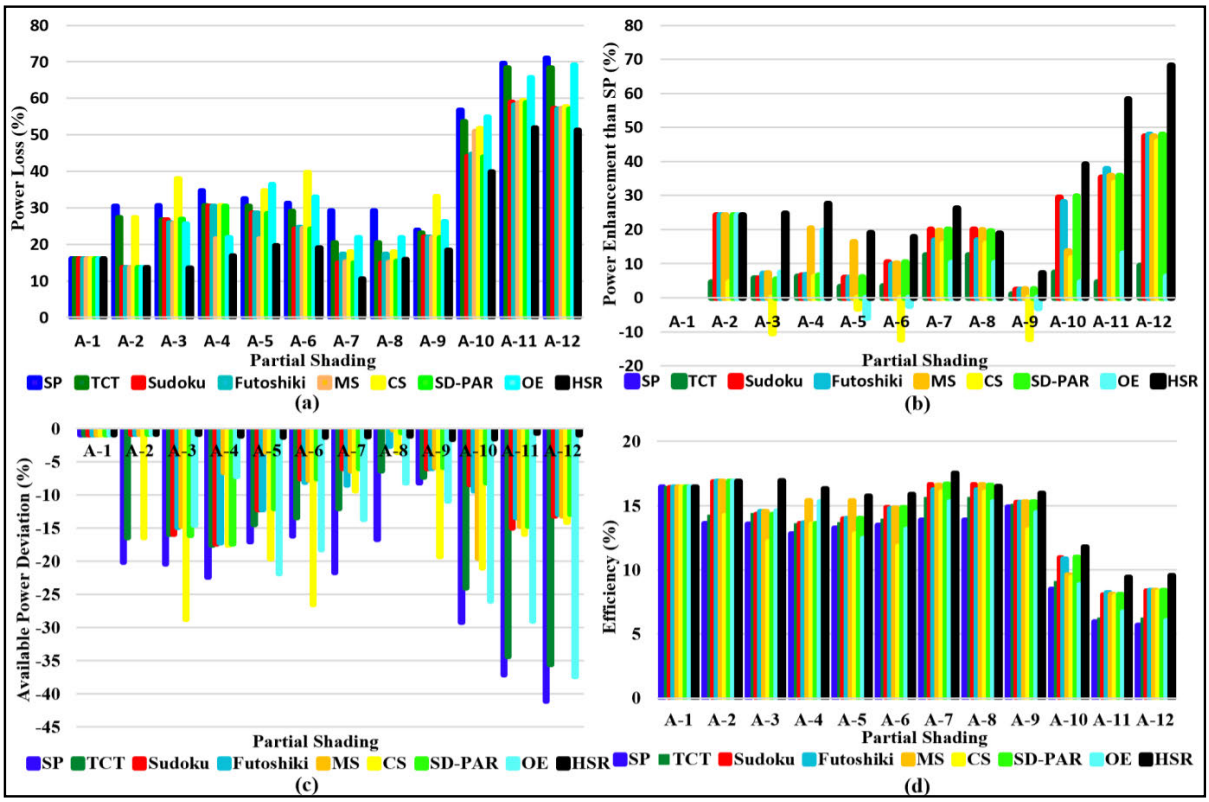

FIGURE 9. Graphical comparison of various parameters of different 5 × 5 PV array techniques with HSR. (a) Power loss (%), (b) Power enhancement than SP, (c) Available power deviation (%), and (d) efficiency.

SD-PAR (5.17 kW and $14.50P_r$) and MS (5.17kW and $14.40P_r$). From the P-V curves given in FIGURE 8 (c), it can be seen that the HSR has a convex curve whereas other techniques exhibited distorted curves with multiple peaks. Also, HSR has a higher efficiency of 15.98% than the SP (14.91%), TCT (15.06%), Sudoku (15.27%), Futoshiki (15.27%), MS (15.30%), CS (13.11%), SD-PAR (15.30%) and OE (14.47%).

10) CASE A10 (76% SHADING)

FIGURE 5 (j) shows the shading case A10 and from Table 3, it has been found that HSR has mathematically generated higher power of $11.25P_r$ than TCT ($8.80P_r$), Sudoku ($10.50\,P_r$), Futoshiki ($10.60P_r$), MS ($9P_r$), CS ($9P_r$), SD-PAR ($10.50P_r$) and OE ($8.40P_r$). The P-V curves generated by different techniques have been depicted in FIGURE 8 (d) in which HSR has exhibited convex characteristics as compared to others. Also, the power output of HSR (3.98kW) is higher than the SP (2.86kW), TCT (3.07kW), Sudoku (3.70kW), Futoshiki (3.66kW), MS (3.25kW), CS (3.19kW), SD-PAR (3.71kW) and OE (2.99kW). Also, the power deviation in the SP, TCT, Sudoku, Futoshiki, MS, CS, SD-PAR, OE, and HSR have been calculated as -29.21%, -24.01%, -8.42%, -9.41%, -19.55%, -21.04%, -8.17%, -25.99% and -1.49%.

11) CASE A11 (84% SHADING)

FIGURE 5 (k) shows the shading case A11 and from the calculation in TABLE 3, the theoretical power of the HSR has been found higher i.e., $9P_r$ than the TCT ($6P_r$), Futoshiki ($7.5P_r$), MS ($7.5P_r$), CS ($7.5P_r$), SD-PAR ($7P_r$) and OE ($6P_r$). FIGURE 8 (e) shows the P-V curves of different array techniques where HSR has a higher power output of 3.18kW with a convex curve whereas SP (2.01kW), TCT (2.10kW), Sudoku (2.72kW), Futoshiki (2.77kW), MS (2.73kW), CS (2.69kW), SD-PAR (2.73kW) and OE (2.27kW) has multiple power peaks in their curves. As compared to SP, HSR has a power enhancement of 58.21% whereas the value lies at 4.48 % for TCT, 35.32% for Sudoku, 37.81% for Futoshiki, 35.82 % for MS, 33.83% for CS, 35.82% for SD-PAR and 12.94% for OE.

12) CASE A12 (92% SHADING)

The shading case in FIGURE 5 (l) shows the most of the modules are operating under shading with multiple irradiance levels. The theoretical power calculation of different array techniques has been performed in TABLE 3 in which HSR generated a higher value of $8.50P_r$ with reduced difference in row currents.

Also, the P-V curves in FIGURE 8 (f) show that HSR has higher power output of 3.23kW as compared to the

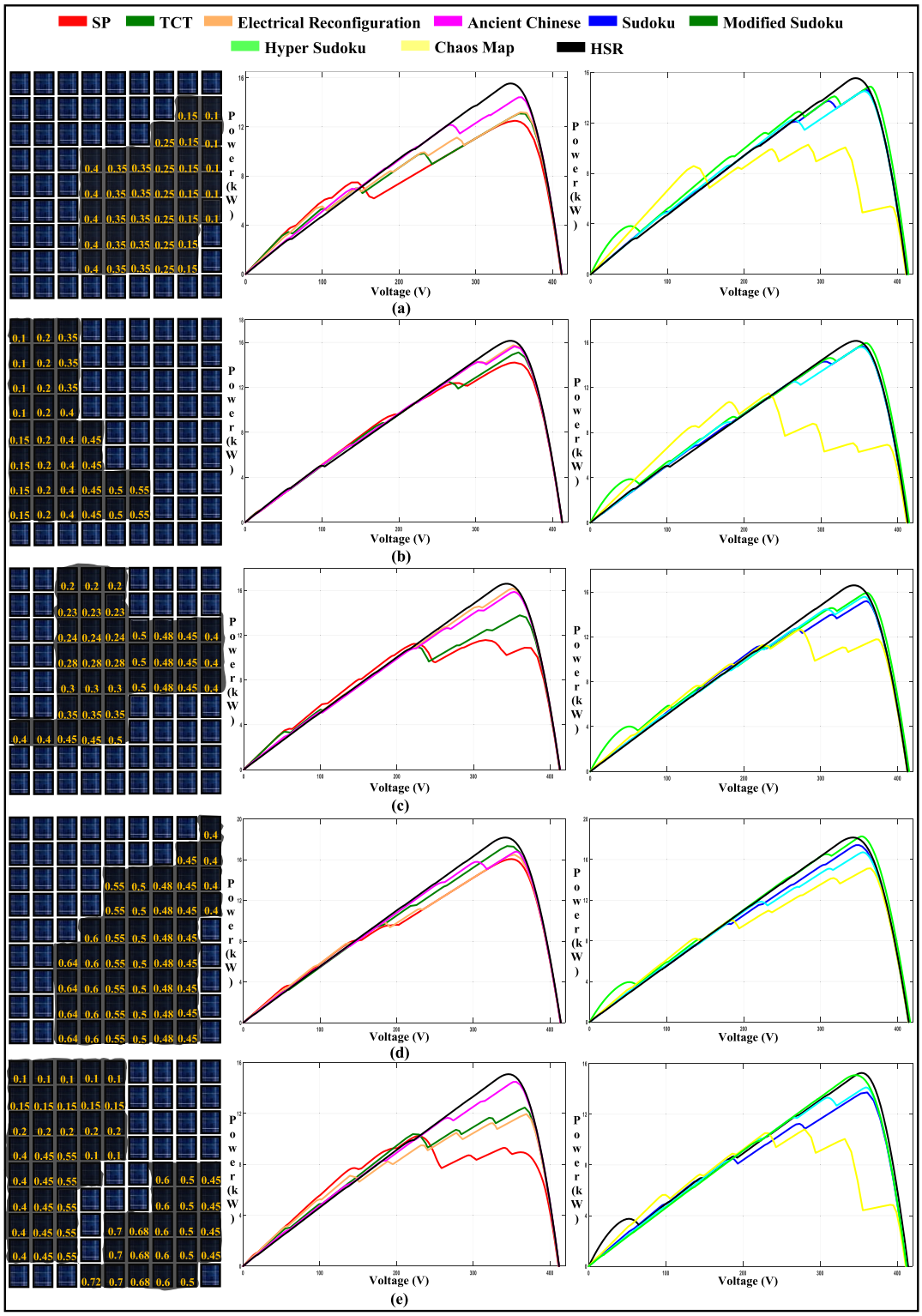

FIGURE 10. Performance of different 9 × 9 PV array techniques under partial shading case (a) B1, (b) B2, (c) B3, (d) B4, and (e) B5.

SP (1.92kW), TCT (2.1kW), Sudoku (2.83kW), Futoshiki (2.84kW), MS (2.83kW), CS (2.80kW), SD-PAR (2.84kW) and OE (2.04kW). Also, HSR has a 68.23% higher power output than SP with a lower power deviation of -0.92 %.

The detailed summarized results of the 5 × 5 PV array with different techniques and HSR have been presented in TABLE 4. It can be observed that, in every case, HSR excelled in performance in terms of lower power

Algorithm 1 Pseudo-Code for HSR Algorithm for PV Array Reconfiguration

1: Initialize parameters: Harmony memory size (HMS), pitch adjustment ratio (PAR) and Maximum Iterations (Max_itr).
2: Initialize the PV array of size (row * colm).
3: Record irradiance level for (row * colm) is calculated using

$$I_{Mij} = \left(\frac{S_{ij}}{S_n}\right) \times I_M$$

4: Calculate Voltage and current for each row. Using KVL formula and the voltage of each array is calculated

$$V_a = \sum_{k=2}^{k=r} V_{mk}$$

5: Calculate PV Power for all agents using Objective Function.

$$MaximizeF(i) = \sum(p) + \left(\frac{W_e^2}{E_r}\right) + \left(W_p^2 \times P_a\right)$$

$$\sum(p) = \sum_{k=1}^{9} I_r V_r$$

$$E_r = \sum_{r=1}^{9} |I_M - I_r|^2$$

Where I_M, I_r, V_r and E_r denote the maximum allowed value of the current being bypassed, current, voltage limit and current value difference respectively.
6: Short the power in descending order and store best solution.
7: **While** (Current_itr< Max_itr) **do**
8: **While** (i ≤ number of variables) textbf do
9: **If** (rand < HMCR)
10: Select value from Harmony from Harmony Memory for variable i.
11: **If** (rand < PAR) **do**
12: Perform pitch adjustment on selected harmony.
13: **End if**
14: **Else**
15: Choose a random value
16: **End While**
17: Evaluate Fitness value for New Harmony.
18: Compare new harmony and save it if it is better.
19: **End While**
20: Retum the best harmony available from the harmony memory.

loss, higher efficiency, lower peak count, and actual power deviation.

The graphical comparison of various parameters of the 5 × 5 PV arrays has been done in FIGURE 9 from which it can be observed that the HSR has shown higher performance in terms of reducing the power loss, enhancing the power output, generating maximum power from the available power with higher efficiency.

B. ANALYSIS USING 9 × 9 PV ARRAY

The proposed HSR has been implemented to a 9 × 9 PV array and compared with SP, TCT, ER [29], ancient Chinese (AC) [30], Sudoku [23], modified Sudoku (MOS) [31], hyper Sudoku (HS) [32] and Chaos Map (CM) [33] techniques under five distinct shading cases (B1 to B5). The shading cases and P-V curves generated by different array techniques along with the HSR have been depicted in FIGURE 10.

During shading case B1 (FIGURE 10 (a)), HSR has higher power output of 15.64kW with 1 peak in the P-V curve as compared to the SP (12.49kW, 2 peaks), TCT (13.09kW, 5 peaks), ER (13.19kW, 6 peaks), AC (14.42kW, 3 peaks), Sudoku (14.64kW, 6 peaks), MOS (14.87kW, 6 peaks), HS (14.51kW, 4 peaks) and CM (10.27 kW, 6 peaks).

During case B2 (FIGURE 10 (b)), the power output by the HSR has been noted to be higher i.e., 16.23kW with 1 peak in the P-V curve than SP (14.2 kW, 3 peaks), TCT (15.1kW, 3 peaks), ER (15.73kW, 3 peaks), AC (15.64kW, 3 peaks), Sudoku (15.68kW, 3 peaks), MOS (15.94kW, 5 peaks), HS (15.58kW, 3 peaks) and CM (10.27kW, 6 peaks).

During case B3 (FIGURE 10 (c)), HSR generated a higher power output of 16.69kW with 1 peak in the P-V curve than SP (11.56kW, 5 peaks), TCT (13.78kW, 5 peaks), ER (16.17 kW, 3 peaks), AC (15.87kW, 5 peaks), Sudoku (15.19kW, 4 peaks), MOS (15.94kW, 7 peaks), HS (15.58kW, 5 peaks) and CM (12.62kW, 7 peaks).

During case B4 (FIGURE 10 (d)), it can be noticed from the P-V curve that HSR has higher power output (19.07kW) with single peak where as other techniques like SP, TCT, ER, AC, Sudoku, MOS, HS and CM with power outputs of 16.06 kW, 17.33kW, 16.49kW, 16.80kW, 17.42kW, 18.28kW, 16.72kW and 15.14kW with peaks count as 4, 1, 5, 3, 5, 4, 4 and 5 respectively.

During case B5 (FIGURE 10 (e)), the maximum power output of HSR has been noted as higher i.e., 15.19kW with single power peak in the P-V curve than SP (10.23kW with 6 peaks), TCT (12.47kW with 5 peaks), ER (11.96kW with 7 peaks), AC (14.48kW with 3 peaks), Sudoku (13.72kW with 4 peaks), MOS (15.26kW with 4 peaks), HS (14.12kW with 5 peaks) and CM (10.81kW with 7 peaks).

Later on, the power generation and peaks of the HSR are compared with GA [39], PSO [40], AVO [41], MHHO [42], DF [43], HB [44], MA [45], GWO [46] and FF [47] reconfiguration techniques under the above shading cases. It has been found that HSR generated nearly equal power output with a single peak compared to the other dynamic techniques during all the cases. The detailed results of power output by different configurations have been given in TABLE 5 in which it can be observed that HSR has higher power output than any static techniques and nearly equal power output than dynamic techniques.

Additionally, to show the operation of the proposed HSR under varying shading in comparison with GA, PSO, AVO, MHHO, DF, HB, MA, GWO, and FF, time-domain analysis has been considered for evaluation using a 9×9 PV array. The arrays with different dynamic reconfigurations along with the

TABLE 5. Power output of different 9 × 9 PV array techniques during shading cases B1 to B5.

Shading Case	*Power Output, Peaks*								
	SP	TCT	ER [29]	Ancient Chinese [30]	Sudoku [23]	Modified Sudoku [31]	Hyper Sudoku [32]	Chaos Map [33]	GA [39]
B1	12.49kW, 2	13.09kW, 5	13.19kW, 6	14.42kW, 3	14.64kW, 6	14.87kW, 6	14.51kW, 4	10.27kW, 6	15.63kW, 1
B2	14.20kW, 3	15.10kW, 3	15.73kW, 3	15.64kW, 3	15.68kW, 3	15.94kW, 5	15.58kW, 3	11.47kW, 6	16.22kW, 1
B3	11.56kW, 5	13.78kW, 5	16.17kW, 3	15.87kW, 5	15.19kW, 4	15.94kW, 7	15.58kW, 5	12.62kW, 7	16.67kW, 1
B4	16.06kW, 4	17.33kW, 1	16.49kW, 5	16.80kW, 3	17.42kW, 5	18.28kW, 4	16.72kW, 4	15.14kW, 5	18.98kW, 1
B5	10.23kW, 6	12.47kW, 5	11.96kW, 7	14.48kW, 3	13.72kW, 4	15.26kW, 4	14.12kW, 5	10.81kW, 7	15.18kW, 1
Shading Case	***Power Output, Peaks***								
	PSO [40]	**AVO [41]**	**MHHO [42]**	**DF [43]**	**HB [44]**	**MA [45]**	**GWO [46]**	**FF [47]**	**HSR**
B1	15.64kW, 1	15.63kW, 1	15.63kW, 1	15.64kW, 1	15.64kW, 1	15.63kW, 1	15.64kW, 1	15.62kW, 1	15.64kW, 1
B2	16.22kW, 1	16.23kW, 1	16.22kW, 1	16.22kW, 1	16.23kW, 1	16.23kW, 1	16.22kW, 1	16.23kW, 1	16.23kW, 1
B3	16.67kW, 1	16.68kW, 1	16.69kW, 1	16.69kW, 1	16.68kW, 1	16.69kW, 1	16.67kW, 1	16.68kW, 1	16.69kW, 1
B4	18.96kW, 1	18.95kW, 1	18.96kW, 1	18.96kW, 1	18.97kW, 1	18.96kW, 1	18.97kW, 1	18.95kW, 1	18.97kW, 1
B5	15.18kW, 1	15.19kW, 1	15.19kW, 1	15.18kW, 1	15.17kW, 1	15.19kW, 1	15.19kW, 1	15.19kW, 1	15.19kW, 1

TABLE 6. Summarized results (Time) of time-domain analysis in 9 × 9 PV array during varying partial shading cases B5-B8.

Shading Case B5						**Shading Case B6**					
	t=0-1s	*t=1-2s*	*t=2-3s*	*t=3-4s*	*t=4-5s*		*t=0-1s*	*t=1-2s*	*t=2-3s*	*t=3-4s*	*t=4-5s*
SP	-	-	-	-	-	**SP**	-	-	-	-	-
GA	No shading	1.20s	2.19s	3.18s	4.17s	**GA**	No shading	1.21s	2.20s	3.19s	4.18s
PSO	No shading	1.18s	2.17s	3.16s	4.15s	**PSO**	No shading	1.19s	2.18s	3.17s	4.16s
AVO	No shading	1.24s	2.26s	3.23s	4.25s	**AVO**	No shading	1.25s	2.26s	3.24s	4.26s
MHHO	No shading	1.27s	2.28s	3.25s	4.27s	**MHHO**	No shading	1.28s	2.29s	3.26s	4.28s
DF	No shading	1.22s	2.24s	3.21s	4.23s	**DF**	No shading	1.23s	2.25s	3.22s	4.24s
HB	No shading	1.19s	2.20s	3.18s	4.19s	**HB**	No shading	1.20s	2.21s	3.19s	4.20s
MA	No shading	1.23s	2.22s	3.21s	4.20s	**MA**	No shading	1.24s	2.23s	3.22s	4.21s
GWO	No shading	1.21s	2.19s	3.19s	4.18s	**GWO**	No shading	1.22s	2.20s	3.20s	4.19s
FF	No shading	1.17s	2.16s	3.15s	4.14s	**FF**	No shading	1.18s	2.17s	3.16s	4.16s
HSR	No shading	1.10s	2.12s	3.11s	4.13s	**HSR**	No shading	1.11s	2.13ss	3.12s	4.14s
Shading Case B8						**Shading Case B8**					
	t=0-1s	*t=1-2s*	*t=2-3s*	*t=3-4s*	*t=4-5s*		*t=0-1s*	*t=1-2s*	*t=2-3s*	*t=3-4s*	*t=4-5s*
SP	-	-	-	-	-	**SP**	-	-	-	-	-
GA	No shading	1.20s	2.25s	3.22s	4.24s	**GA**	0.26s	1.28s	2.30s	3.32s	4.34s
PSO	No shading	1.18s	2.22s	3.20s	4.21s	**PSO**	0.24s	1.26s	2.28s	3.30s	4.32s
AVO	No shading	1.24s	2.26s	3.28s	4.30s	**AVO**	0.32s	1.34s	2.36s	3.38s	4.40s
MHHO	No shading	1.28s	2.30s	3.32s	4.34s	**MHHO**	0.26s	1.38s	2.40s	3.42s	4.44s
DF	No shading	1.23s	2.26s	3.27s	4.29s	**DF**	0.30s	1.32s	2.34s	3.36s	4.38s
HB	No shading	1.20s	2.22s	3.24s	4.26s	**HB**	0.27s	1.29s	2.31s	3.33s	4.35s
MA	No shading	1.24s	2.25s	3.26s	4.28s	**MA**	0.31s	1.33s	2.35s	3.37s	4.39s
GWO	No shading	1.22s	2.23s	3.24s	4.26s	**GWO**	0.29s	1.31s	2.33s	3.35s	4.37s
FF	No shading	1.18s	2.19s	3.20s	4.22s	**FF**	0.25s	1.27s	2.29s	3.31s	4.33s
HSR	No shading	1.14s	2.12s	3.15s	4.13s	**HSR**	0.16s	1.18s	2.20s	3.21s	4.24s

TABLE 7. Comparison of harmony search (HS) technique with existing algorithms.

Parameters	*Algorithms for PV Array Reconfiguration*									
	HS	**GA**	**PSO**	**AVO**	**MHHO**	**DF**	**HB**	**MA**	**GWO**	**FF**
Simplicity	High	Medium	Medium	High	Medium	Medium	High	High	High	High
Convergence	High	Medium	Medium	Medium	Medium	High	Medium	High	Medium	Medium
Diversification	High	Medium	High	Medium	High	High	Medium	Medium	Medium	High
Local Search	Built-in	RC	RC	Built-in	RC	RC	RC	RC	RC	RC
Memory Usage	Low	Medium	Medium	Medium	Medium	Medium	Medium	Medium	Medium	Medium
Flexibility	High	Medium	Medium	High	High	High	High	High	Medium	Medium
Robustness	High	Medium	Medium	Medium	Medium	Medium	Medium	Medium	High	Medium
Adaptability	High	Medium	Medium	Medium	Medium	Medium	Medium	Medium	Medium	Medium
Parallelization	High	Medium	Medium	Medium	Medium	Medium	Medium	Medium	Medium	Medium

**RC-Required Customization*

HSR have been operated for a duration of *t=5s* where there is a change in the shading in terms of pattern, size, and strength in every *1s* duration. The varying shading cases B5, B6, B7, and B8 have been depicted in FIGURE 11 in which it can be noted that the PV array operates under multiple shading cases during the simulation time i.e., t=0-5s.

During shading case B5 (shown in FIGURE 11 (a)), the array operates under normal scenarios during t=0-1s

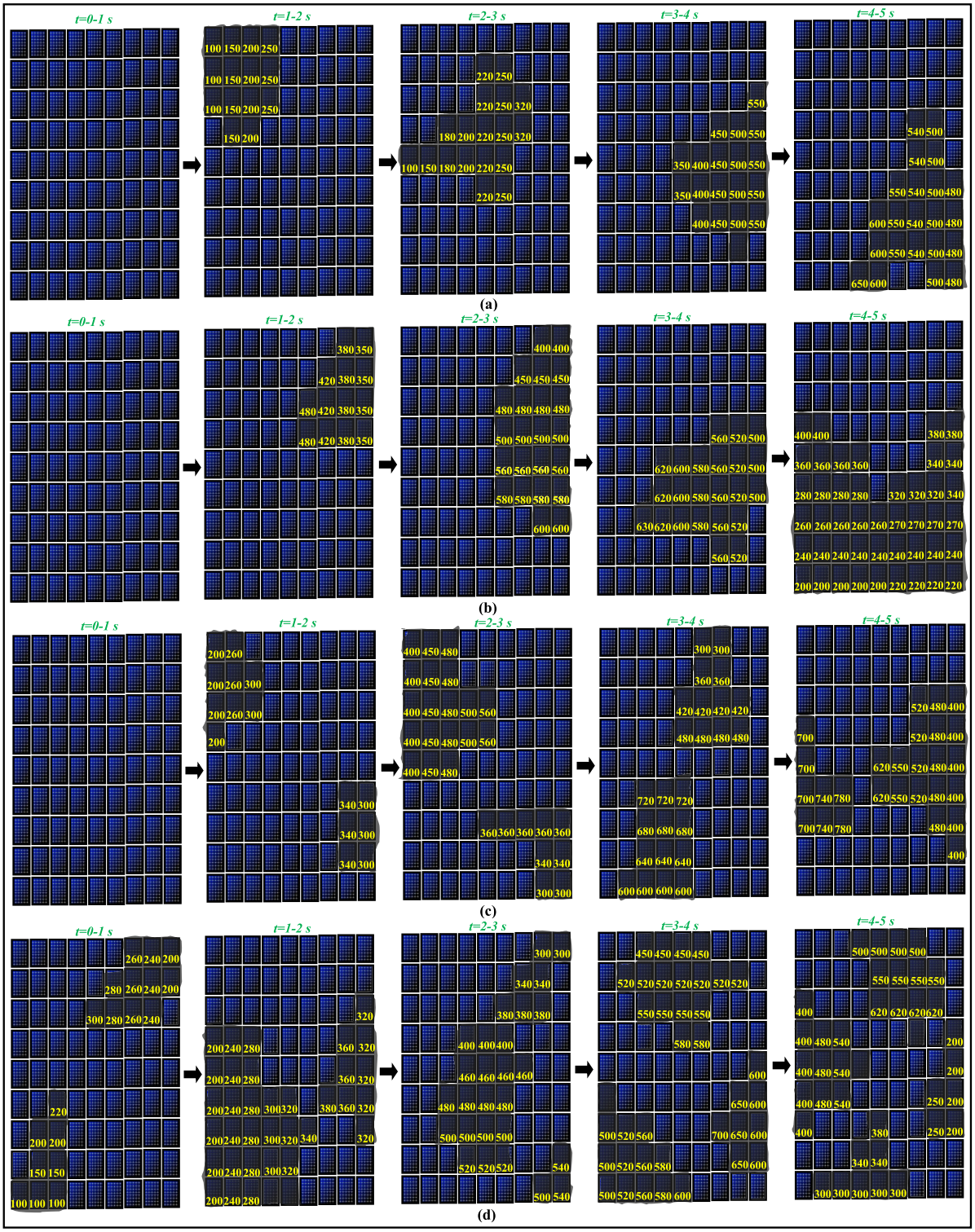

FIGURE 11. Performance of different 9 × 9 PV array techniques under partial shading case (a) B1, (b) B2, (c) B3, (d) B4, and (e) B5.

with all the techniques generating the same power of 21.55kW. At t=1s, the arrays encounter shading with multiple irradiance levels of 800W/m^2, 100W/m^2, 150W/m^2, 200W/m^2 and 250 W/m^2 and continues till t=2s. During this shading, the power outputs of all the techniques have been noted to be the same i.e., 15.78kW whereas SP has a lower power output of 11.72kW. From the power output graph presented in FIGURE 12 (a), it can be observed that HSR has enhanced the power output through optimal reconfiguration at t=1.10s as compared to

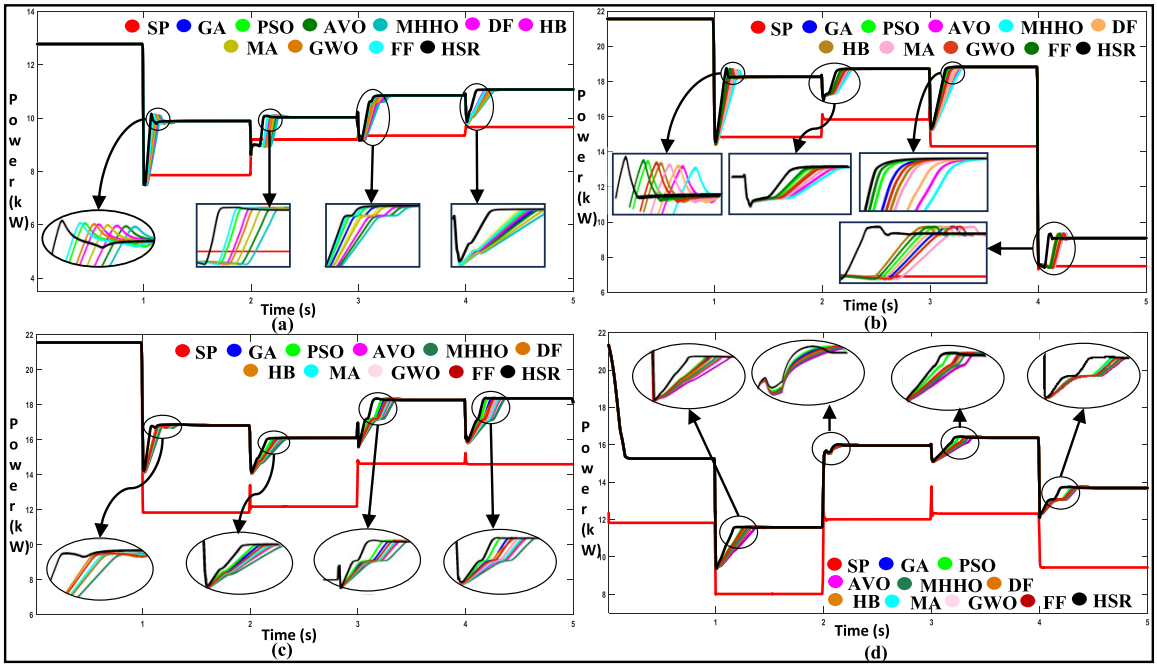

FIGURE 12. Time-domain power generation of SP, GA, PSO, AVO, MHHO, DF, HB, MA, GWO, FF, and HSR during the varying shading case (a) B5, (b) B6, (c) B7 and (d) B8.

TABLE 8. Performance of 9 × 5 PV array techniques during various shading cases.

Shading Case	Shading Scenario	Power Output
C1		**SP-** 8.07kW **TCT-** 8.52kW **FER-** 8.64kW **HSR-** 10.29kW
C2		**SP-** 7/10kW **TCT-** 7.69kW **FER-** 7.99kW **HSR-** 9.34kW
C3	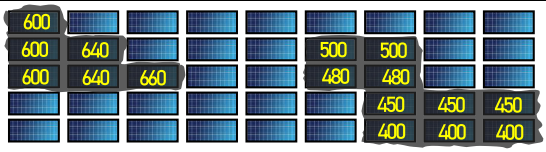	**SP-** 8.26kW **TCT-** 9.33kW **FER-** 9.36kW **HSR-** 10.84kW
C4		**SP-** 6.76kW **TCT-** 8.71kW **FER-** 8.84kW **HSR-** 9.86kW
C5		**SP-** 4.93kW **TCT-** 6.65kW **FER-** 7.46kW **HSR-** 8.40kW

the GA (t=1.20s), PSO (t=1.18s), AVO (t=1.24s), MHHO (t=1.27s), DF (t=1.22s), HB (t=1.19s), MA (t=1.23s), GWO (t=1.21s) and FF(t=1.17s). The shading changes at t=2s with irradiance levels of 800W/m^2, 100W/m^2, 150W/m^2, 180W/m^2, 200W/m^2, 220W/m^2, 250 W/m^2, and 320W/m^2 and continues till t=3s. During this shading, SP has

TABLE 9. Experimental analysis of 3 × 3 PV array under partial shading D1 and D2.

Shading Case	Shading Scenario	Legend	P-V Curves	Power Output	
D1	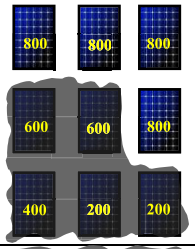	SP TCT	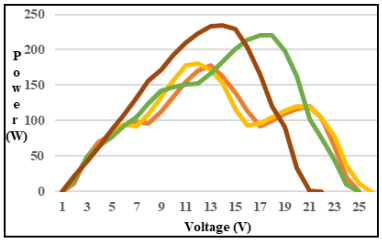	SP	178.7W
				TCT	181.9W
				SDS	221.2W
				HSR	236.2W
D2	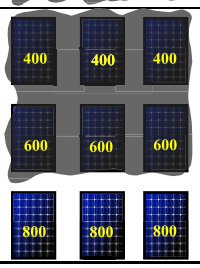	SDS HSR	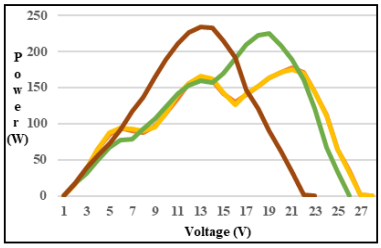	SP	164.8W
				TCT	165.2W
				SDS	224.3W
				HSR	238W

a lower power output i.e., 14.40kW whereas all the other techniques have equal outputs of 16.05kW.The HSR enhanced power generation of the array at t=2.12s whereas GA, PSO, AVO, MHHO, DF, HB, MA, GWO and FF have enhanced at t=2.19s, t=2.17s, t=2.26s, t=2.28s, t=2.24s, t=2.20s, t=2.22s, t=2.19s and t= 2.16s respectively. The shading again changes at t=3-4s with irradiances of 800 W/m^2, 350W/m^2, 400W/m^2, 450W/m^2, 500W/m^2, and 550 W/m^2. The SP has lower power output of 14.68kW whereas all the dynamic reconfiguration generated equal power of 17.69kW. The HSR has enhanced the power output within less time i.e., t=3.11s whereas GA, PSO, AVO, MHHO, DF, HB, MA, GWO, and FF generated higher power at t=3.18s, 3.16s, 3.23s, 3.25s, 3.21s, 3.18s, 3.21s, 3.18s and 3.15s respectively. The shading changes at t=4s with irradiance levels of 800W/m^2, 480W/m^2, 500W/m^2, 540W/m^2, 550 W/m^2, 600 W/m^2, and 650W/m^2. The power output of SP has been noted as 15.23kW whereas all other reconfiguration techniques generated 18.14kW during this scenario. The HSR has done power enhancement at t=4.13s that indicates higher convergence speed than GA (*t=4.17s*), PSO (*t=4.15s*), AVO (*t=4.25s*), MHHO (*t=4.27s*), DF (*t=4.23s*), HB (*t=4.19s*), MA (*t=4.20s*), GWO (*t=4.18s*) and FF (*t=4.14s*).Similarly, during shading case B6 (FIGURE 11 (b)), the arrays operate at normal scenarios from t=0-1s and encounter multiple partial shading scenarios from t=1-4s. The power output graphs presented in FIGURE (b) shows that SP has lower power output during t=1-2s (14.83kW), t=2-3s (15.76kW), t=3-4s (14.30kW) and t=4-5s (7.48kW) whereas GA, PSO, AVO, MHHO, DF, HB, MA, GWO, FF and HSR has generated equal higher power output of 18.26kW, 18.72kW, 18.82kW and 9.67kW during t=1-2s, t=2-3s, t=3-4s and t=4-5s respectively. It has been noted that the HSR calculated the optimal reconfiguration within a very less time i.e., t=1.11s, t=2.13s, t=3.12s, and t=4.14s than GA (t=1.21s, t=2.20s, t=3.19s and t=4.18s), PSO (t=1.19s, t=2.18s, t=3.17s and t=4.16s), AVO (t=1.25s, t=2.26s, t=3.24s and t=4.26s), MHHO (t=1.28s, t=2.29s, t=3.26s and t=4.28s), DF (t=1.23s, t=2.25s, t=3.22s and t=4.24s), HB (t=1.20s, t=2.21s, t=3.19s and t=4.20s), MA (t=1.24s, t= 2.23s, t=3.22s and t=4.21s), GWO (t=1.22s, t=2.20s, t=3.20s and t=4.19s) and FF (t=1.18s, t=2.17s, t=3.16s and t=4.16s).

During shading B7 (FIGURE 11 (b)), the power output of SP has been noted to be lower i.e., 11.83kW, 12.17kW, 14.63 kW and 14.59kW whereas other techniques generated equal power outputs of 16.81kW, 16.10kW, 18.26kW and 18.38 kW during t=1-2s, t=2-3s, t=3-4s and t=4-5s respectively. From the power output graph shown in FIGURE 12 (c), it can be observed that HSR has a faster response in terms of power enhancement as compared to other techniques. The power enhancement time of HSR has been noted as t=1.14s, t=2.12s, t=3.15s and t=4.14s which is lower than GA (t =1.20s, t=2.25s, t=3.22s and t=4.24s), PSO (t=1.18s, t=2.22s, t=3.20s and t=4.121s), AVO (t=1.24s, t=2.26s, t=3.28s and t=4.30s), MHHO (t=1.28s, t=2.30s, t=3.32s and t=4.34s), DF (t=1.23s, t=2.26s, t=3.27s and t=4.29s), HB (t=1.20s, t=2.22s, t=3.24s and t=4.26s), MA (t=1.24s, t= 2.25s, t=3.26s and t=4.28s), GWO (t=1.22s, t=2.23s, t=3.24s and t=4.26s) and FF (t=1.18s, t=2.19s, t=3.20s and t=4.22s) during shading occurring at t=1-2s, t=2-3s, t=3-4s and t=4-5s respectively.

The summarized results of the time-domain analysis for shading cases B5-B8 have been given in Table 6. From the table, it can be observed that HSR has faster convergence (ability to calculate the optimal reconfiguration) during all the shading scenarios as compared to other algorithms. Also, from the above analysis, it is noted that all the algorithms generated equal power during shading however, the response (power enhancement) time differs from each other. The

average optimal reconfiguration calculation time of the GA, PSO, AVO, MHHO, DF, HB, MA, GWO, FF and HSR have been calculated as 0.23s, 0.21s, 0.29s, 0.31s, 0.27s, 0.24s, 0.27s, 0.25s, 0.21s and 0.15s respectively.

A comparison of the harmony search (HS) technique with other techniques such as GA, PSO, AVO, MHHO, DF, HB, MA, GWO, and FF in terms of various parameters has been done in TABLE 7. From the table, it can be observed that the HS algorithm has numerous advantages in terms of simplicity, diversification, convergence, memory usage, local search, flexibility, robustness, adaptability, etc. Also, from the above analysis under partial shading for 9×9 array, it has been found that HSR has shown similar performance to other techniques.

In addition, the HSR has been tested using a 9×4 PV array (unsymmetrical) and compared with SP, TCT, and FER [34] under five distinct shading cases. The shading scenario and power output by different techniques have been summarized in TABLE 8. It has been found that HSR has higher power outputs of 10.29kW, 9.34kW, 10.84kW, 9.86kW, and 8.40kW during shading cases C1, C2, C3, C4, and C5 whereas SP has a lower output of 8.07kW, 7.10kW, 8.26kW and 6.76 kW and 4.93kW respectively. The power output of TCT and FER has been found as 8.52kW and 8.64kW during case C1, 7.69kW and 7.99kW during case C2, 9.33kW, and 9.36 kW during case C3, 8.71kW and 8.84kW during case C4 and 6.65kW and 7.46kW respectively.

C. EXPERIMENTAL VALIDATION USING 3 × 3 ARRAY

Later on, an experimental investigation has been carried out to show the application of the proposed HSR in a real-time environment. The experiment has been conducted on the roof of Renewable Energy Lab, SOA University located at Bhubaneswar, India with 20°16′ N and 85°50′ E as latitude and longitude respectively. The average irradiance received by the experimental site during December has been noted as 893W/m^2. The experimental analysis has been carried out using a 3 × 3 array using PV modules with rating as 50W (maximum power), 21.5V (open-circuit voltage), 17.4V (maximum voltage), 3.1A (short-circuit current) and 2.86A (maximum current). The experimental setup is displayed in FIGURE 13 which consists of nine modules, a solar power meter to measure the irradiance received by modules, a multimeter, a voltmeter, and a variable load to plot the P-V curves. The irradiance of modules has been reduced by using layers of transparent color sheets that act as partial shading in the array. Later on, after performing the experiments, P-V curves are plotted using the power and voltage data points.

The detailed experimental results such as shading cases D1 and D2 along with the P-V curves and power outputs have been summarized in Table 9. The HSR has been operated manually by changing the electrical connection of the array based on the reconfiguration provided by the proposed algorithm and compared with SP, TCT, and shade dispersion scheme (SDS) [53] using two shading cases. During shading case D1, HSR generated a significantly higher power output

FIGURE 13. Experimental setup of a 3 × 3 PV array.

of 236.2W as compared to the SP (178.7W), TCT (181.9W), and SDS (221.2W). Similarly, during shading case D2, the HSR showed better performance by generating a higher power output of 238W than SP (164.8W), TCT (165.2), and SDS (224.3W). Also, from the P-V curves obtained from the experiments (in TABLE 9), it can be observed that the HSR has generated the curves with single peaks whereas other techniques exhibited multiple peaks. It is to be noted that there may exist some uncertainty in the experimental data due to various unavoidable factors like fluctuating irradiance, module temperature difference, internal mismatches, and wire losses. Hence, from the above experimental analysis, it can be stated that HSR has effective shade dispersion capability and can be implemented in real-time practical applications for power enhancement from the arrays during partial shading.

From the above analysis, the HSR technique has been found to have a higher performance than existing techniques for all the array sizes under partial shading. In the 5×5 array, HSR has 29.84%, 21.53%, 9.20%, 9.70%, 8.33%, 19.74%, 9.18%, and 20.78% higher power than the SP, TCT, Sudoku, Futoshiki, Magic Square (MS), Competence Square (CS), SD-PAR and Odd-Even (OE) techniques respectively. In the 9 × 9 array, HSR has a power enhancement of 30.22%, 15.99%, 13.52%, 7.16 %, 8.08%, 3.11%, 8.14%, and 18.50% than SP, TCT, ER, Ancient Chinese (AC), Sudoku, Modified Sudoku (MOS), Hyper Sudoku (HS) and Chaos Map (CM) respectively. For the 9 × 5 array, the HSR has 41.31%, 19.59%, and 15.19% higher power than SP, TCT and FER. Additionally, HSR has shown nearly equal performance to the GA, PSO, AVO, MHHO, DF, HB, MA, GWO, and FF techniques in terms of power generation. The time-domain investigation reveals that the HSR has a higher convergence speed i.e., the ability to calculate and reconfigure the PV array with varying shading scenarios as compared to others. The average optimal reconfiguration time of the GA, PSO, AVO, MHHO, DF, HB, MA, GWO, FF, and HSR have been calculated as 0.23s, 0.21s, 0.29s, 0.31s, 0.27s, 0.24s, 0.27s, 0.25s, 0.21s and 0.15s respectively. This efficiency can be attributed to HSR due to its unique improvisation-inspired search mechanism, fostering a harmonious interplay between candidate solutions. The HSR algorithm strikes a balance

between exploration and exploitation, allowing it to swiftly adapt to changing shading scenarios. Also, HSR benefits from a memory structure that efficiently retains promising solutions, aiding quicker convergence. The simplicity of the HSR conceptual framework and its adaptive nature contribute to its agility, making it particularly effective in time-sensitive scenarios like dynamic array reconfiguration. The superior performance of HS in this time domain analysis underscores its suitability for rapid and effective optimization in dynamically changing environments. Additionally, HSR has various other advantages in terms of simplicity, higher diversification, lower memory usage, built-in local search, flexibility, robustness, wide adaptability, and parallelization.

V. CONCLUSION

In this paper, a harmony search reconfiguration (HSR) has been proposed for PV arrays to reduce power losses and enhance power output during partial shading. The HSR has been compared with twenty-two existing conventional, static, and dynamic using three array sizes of 5×5, 9×9, 9×5, and 3×3 (experimental analysis). From, the conducted analysis, the following conclusions have been drawn:

- ➢ HSR has higher power generation during all the partial shading cases for all PV array sizes.
- ➢ In the 5×5 array, HSR has 29.84%, 21.53%, 9.20%, 9.70%, 8.33%, 19.74%, 9.18%, and 20.78% higher power than the SP, TCT, Sudoku, Futoshiki, Magic Square (MS), Competence Square (CS), SD-PAR and Odd-Even (OE) techniques respectively.
- ➢ In the 9×9 array, HSR has a power enhancement of 30.22%, 15.99%, 13.52%, 7.16 %, 8.08%, 3.11%, 8.14%, and 18.50% than SP, TCT, ER, Ancient Chinese (AC), Sudoku, Modified Sudoku (MOS), Hyper Sudoku (HS) and Chaos Map respectively.
- ➢ In the time-domain analysis of 9×9 PV array, HSR has lower average optimal reconfiguration time of 0.15s than GA (0.23s), PSO (0.21s), AVO (0.29s), MHHO (0.31s), DF (0.27s), HB (0.24s), MA (0.27 s), GWO (0.25s), and FF (0.21s) indicating higher convergence and calculation speed of HSR.
- ➢ In the 9×5 array, HSR has power enhancement of 41.31%, 19.59%, and 15.19% higher power than SP, TCT, and FER respectively.
- ➢ In the 3×3 PV array, experimental results show the higher power generation of the HSR during partial shading than other techniques.
- ➢ HSR has an average power enhancement of 24.64% and 11.28% as compared to conventional and static techniques.
- ➢ HSR generated nearly equal power as compared to dynamic techniques like genetic algorithm, particle swarm optimization, African vultures optimization, modified Harris hawks optimizer, dragonfly, honey badger, grey wolf optimization, firefly and Munkres assignment with advantages like simplicity, higher convergence, higher diversification, lower memory usage, built-in local search, flexible, robust, wide adaptability and parallelization.
- ➢ HSR has a lower average actual power deviation of -1.10% as compared to SP (-20.94%), TCT (-16.54 %), Sudoku (-8.63%), Futoshiki (-8.93%), Magic Square (-7.85%), Competence Square (-16.10%), SD-PAR (-8.58%) and Odd-Even in 5×5 array.
- ➢ HSR is easy to implement in symmetrical and un-symmetrical PV arrays with a simple algorithm and reduced switch count.
- ➢ HSR ensures higher power output with smooth P-V curves during partial shading scenarios with higher efficiency

Hence, the proposed HSR technique can be an effective solution for the reliable operation of solar PV arrays that can be implemented in arbitrary sizes and have wide application in roof-top and grid-connected PV systems ensuring efficient power generation during partial shading. The reduction of switches and the design of simpler algorithms can be the potential future scope of this work.

REFERENCES

[1] K. Abdulmawjood, S. Alsadi, S. S. Refaat, and W. G. Morsi, "Characteristic study of solar photovoltaic array under different partial shading conditions," *IEEE Access*, vol. 10, pp. 6856–6866, 2022.

[2] A. K. Singhal, N. S. Beniwal, R. Beniwal, and K. Lalik, "An experimental study of drift caused by partial shading using a modified DC-(P&O) technique for a stand-alone PV system," *Energies*, vol. 15, no. 12, p. 4251, Jun. 2022.

[3] R. Ahmad, A. F. Murtaza, H. A. Sher, U. T. Shami, and S. Olalekan, "An analytical approach to study partial shading effects on PV array supported by literature," *Renew. Sustain. Energy Rev.*, vol. 74, pp. 721–732, Jul. 2017.

[4] M. Dhimish and A. M. Tyrrell, "Power loss and hotspot analysis for photovoltaic modules affected by potential induced degradation," *NPJ Mater. Degradation*, vol. 6, no. 1, p. 11, Feb. 2022.

[5] M. Sarvi and A. Azadian, "A comprehensive review and classified comparison of MPPT algorithms in PV systems," *Energy Syst.*, vol. 13, no. 2, pp. 281–320, May 2022.

[6] M. Kermadi, Z. Salam, A. M. Eltamaly, J. Ahmed, S. Mekhilef, C. Larbes, and E. M. Berkouk, "Recent developments of MPPT techniques for PV systems under partial shading conditions: A critical review and performance evaluation," *IET Renew. Power Gener.*, vol. 14, no. 17, pp. 3401–3417, Dec. 2020.

[7] B. Yang, T. Zhu, J. Wang, H. Shu, T. Yu, X. Zhang, W. Yao, and L. Sun, "Comprehensive overview of maximum power point tracking algorithms of PV systems under partial shading condition," *J. Cleaner Prod.*, vol. 268, Sep. 2020, Art. no. 121983.

[8] D. J. K. Kishore, M. R. Mohamed, K. Sudhakar, and K. Peddakapu, "Swarm intelligence-based MPPT design for PV systems under diverse partial shading conditions," *Energy*, vol. 265, Feb. 2023, Art. no. 126366.

[9] B. Yang, S. Wu, J. Huang, Z. Guo, J. Wang, Z. Zhang, R. Xie, H. Shu, and L. Jiang, "Salp swarm optimization algorithm based MPPT design for PV-TEG hybrid system under partial shading conditions," *Energy Convers. Manage.*, vol. 292, Sep. 2023, Art. no. 117410.

[10] I. Sajid, A. Gautam, A. Sarwar, M. Tariq, H.-D. Liu, S. Ahmad, C.-H. Lin, and A. E. Sayed, "Optimizing photovoltaic power production in partial shading conditions using dandelion optimizer (DO)-based MPPT method," *Processes*, vol. 11, no. 8, p. 2493, Aug. 2023.

[11] A. G. Abo-Khalil, I. I. El-Sharkawy, A. Radwan, and S. Memon, "Influence of a hybrid MPPT technique, SA-P&O, on PV system performance under partial shading conditions," *Energies*, vol. 16, no. 2, p. 577, Jan. 2023.

[12] R. Celikel, M. Yilmaz, and A. Gundogdu, "A voltage scanning-based MPPT method for PV power systems under complex partial shading conditions," *Renew. Energy*, vol. 184, pp. 361–373, Jan. 2022.

[13] S. K. Vankadara, S. Chatterjee, P. K. Balachandran, and L. Mihet-Popa, "Marine predator algorithm (MPA)-based MPPT technique for solar PV systems under partial shading conditions," *Energies*, vol. 15, no. 17, p. 6172, Aug. 2022.

[14] A. M. Nassef, E. H. Houssein, B. E.-D. Helmy, and H. Rezk, "Modified honey badger algorithm based global MPPT for triple-junction solar photovoltaic system under partial shading condition and global optimization," *Energy*, vol. 254, Sep. 2022, Art. no. 124363.

[15] K. Osmani, A. Haddad, H. Jaber, T. Lemenand, B. Castanier, and M. Ramadan, "Mitigating the effects of partial shading on PV system's performance through PV array reconfiguration: A review," *Thermal Sci. Eng. Prog.*, vol. 31, Jun. 2022, Art. no. 101280.

[16] S. Anjum and V. Mukherjee, "Static and dynamic reconfiguration strategies for reducing partial shading effects in photovoltaic array: A comprehensive review," *Energy Technol.*, vol. 10, no. 7, Jul. 2022, Art. no. 2200098.

[17] V. Gautam, S. Khatoon, and M. F. Jalil, "A review on various mathematical based static reconfiguration strategies to improve generated power under partial shading conditions," in *Proc. Int. Conf. Recent Adv. Electr., Electron. Digit. Healthcare Technol. (REEDCON)*, May 2023, pp. 25–30.

[18] Z. Yang, N. Zhang, J. Wang, Y. Liu, and L. Fu, "Improved non-symmetrical puzzle reconfiguration scheme for power loss reduction in photovoltaic systems under partial shading conditions," *Sustain. Energy Technol. Assessments*, vol. 51, Jun. 2022, Art. no. 101934.

[19] A. Fathy, D. Yousri, T. S. Babu, and H. Rezk, "Triple X sudoku reconfiguration for alleviating shading effect on total-cross-tied PV array," *Renew. Energy*, vol. 204, pp. 593–604, Mar. 2023.

[20] S. Anjum, V. Mukherjee, and G. Mehta, "Addition progression structure photovoltaic array reconfiguration technique to generate maximum power under static partial shading condition," *Arabian J. Sci. Eng.*, vol. 47, no. 11, pp. 14105–14118, Nov. 2022.

[21] D. Yousri, A. Fathy, and E. F. El-Saadany, "Four square sudoku approach for alleviating shading effect on total-cross-tied PV array," *Energy Convers. Manage.*, vol. 269, Oct. 2022, Art. no. 116105.

[22] R. D. Amar Raj and K. Anil Naik, "A generalized Henon map-based solar PV array reconfiguration technique for power augmentation and mismatch mitigation," *IETE J. Res.*, vol. 69, no. 11, pp. 8404–8422, Nov. 2023.

[23] B. I. Rani, G. S. Ilango, and C. Nagamani, "Enhanced power generation from PV array under partial shading conditions by shade dispersion using Su do Ku configuration," *IEEE Trans. Sustain. Energy*, vol. 4, no. 3, pp. 594–601, Jul. 2013.

[24] H. S. Sahu, S. K. Nayak, and S. Mishra, "Maximizing the power generation of a partially shaded PV array," *IEEE J. Emerg. Sel. Topics Power Electron.*, vol. 4, no. 2, pp. 626–637, Jun. 2016.

[25] G. H. K. Varma, V. R. Barry, and R. K. Jain, "A novel magic square based physical reconfiguration for power enhancement in larger size photovoltaic array," *IETE J. Res.*, vol. 69, no. 7, pp. 4644–4657, Sep. 2023.

[26] D. Kumar and R. Raushan, "An innovative competence square technique for PV array reconfiguration under partial shading conditions," *Int. J. Model. Simul.*, pp. 1–16, Jan. 2023.

[27] P. R. Satpathy, R. Sharma, and S. Dash, "An efficient SD-PAR technique for maximum power generation from modules of partially shaded PV arrays," *Energy*, vol. 175, pp. 182–194, May 2019.

[28] S. S. Reddy and C. Yammani, "Odd-even-prime pattern for PV array to increase power output under partial shading conditions," *Energy*, vol. 213, Dec. 2020, Art. no. 118780.

[29] P. S. Rao, G. S. Ilango, and C. Nagamani, "Maximum power from PV arrays using a fixed configuration under different shading conditions," *IEEE J. Photovolt.*, vol. 4, no. 2, pp. 679–686, Mar. 2014.

[30] R. K. Pachauri, S. B. Thanikanti, J. Bai, V. K. Yadav, B. Aljafari, S. Ghosh, and H. H. Alhelou, "Ancient Chinese magic square-based PV array reconfiguration methodology to reduce power loss under partial shading conditions," *Energy Convers. Manage.*, vol. 253, Feb. 2022, Art. no. 115148.

[31] K. Rajani and T. Ramesh, "Maximum power enhancement under partial shadings using a modified sudoku reconfiguration," *CSEE J. Power Energy Syst.*, vol. 7, no. 6, pp. 1187–1201, Nov. 2021.

[32] S. Anjum, V. Mukherjee, and G. Mehta, "Hyper SuDoKu-based solar photovoltaic array reconfiguration for maximum power enhancement under partial shading conditions," *J. Energy Resour. Technol.*, vol. 144, no. 3, Mar. 2022, Art. no. 031302.

[33] V. M. R. Tatabhatla, A. Agarwal, and T. Kanumuri, "A chaos map based reconfiguration of solar array to mitigate the effects of partial shading," *IEEE Trans. Energy Convers.*, vol. 37, no. 2, pp. 811–823, Jun. 2022.

[34] P. R. Satpathy and R. Sharma, "Power and mismatch losses mitigation by a fixed electrical reconfiguration technique for partially shaded photovoltaic arrays," *Energy Convers. Manage.*, vol. 192, pp. 52–70, Jul. 2019.

[35] R. K. Pachauri and J. G. Singh, "Successive rotation approach based novel game puzzles for higher shade dispersion of PV array systems under non-uniform irradiations," *Energy Convers. Manage.*, vol. 276, Jan. 2023, Art. no. 116505.

[36] B. Aljafari, P. K. Balachandran, and T. S. Babu, "Power enhanced solar PV array configuration based on calcudoku puzzle pattern for partial shaded PV system," *Heliyon*, vol. 9, no. 5, May 2023, Art. no. e16041.

[37] V. L. Mishra, Y. K. Chauhan, and K. S. Verma, "A novel reconfiguration of the solar array to enhance peak power and efficiency under partial shading conditions: Experimental validation," *Clean Energy*, vol. 7, no. 4, pp. 824–842, Aug. 2023.

[38] M. S. S. Nihanth, J. P. Ram, D. S. Pillai, A. M. Y. M. Ghias, A. Garg, and N. Rajasekar, "Enhanced power production in PV arrays using a new skyscraper puzzle based one-time reconfiguration procedure under partial shade conditions (PSCs)," *Sol. Energy*, vol. 194, pp. 209–224, Dec. 2019.

[39] D. La Manna, V. Li Vigni, E. Riva Sanseverino, V. Di Dio, and P. Romano, "Reconfigurable electrical interconnection strategies for photovoltaic arrays: A review," *Renew. Sustain. Energy Rev.*, vol. 33, pp. 412–426, May 2014.

[40] G. Sai Krishna and T. Moger, "A novel adaptive dynamic photovoltaic reconfiguration system to mitigate mismatch effects," *Renew. Sustain. Energy Rev.*, vol. 141, May 2021, Art. no. 110754.

[41] S. Li, T. Zhang, and J. Yu, "Photovoltaic array dynamic reconfiguration based on an improved pelican optimization algorithm," *Electronics*, vol. 12, no. 15, p. 3317, Aug. 2023.

[42] Y. Wang and B. Yang, "Optimal PV array reconfiguration under partial shading condition through dynamic leader based collective intelligence," *Protection Control Modern Power Syst.*, vol. 8, no. 1, p. 40, Dec. 2023.

[43] V. L. Mishra, Y. K. Chauhan, and K. S. Verma, "A novel PV array reconfiguration approach to mitigate non-uniform irradiation effect," *Energy Convers. Manage.*, vol. 265, Aug. 2022, Art. no. 115728.

[44] S. N. Deshkar, S. B. Dhale, J. S. Mukherjee, T. S. Babu, and N. Rajasekar, "Solar PV array reconfiguration under partial shading conditions for maximum power extraction using genetic algorithm," *Renew. Sustain. Energy Rev.*, vol. 43, pp. 102–110, Mar. 2015.

[45] T. S. Babu, J. P. Ram, T. Dragicevic, M. Miyatake, F. Blaabjerg, and N. Rajasekar, "Particle swarm optimization based solar PV array reconfiguration of the maximum power extraction under partial shading conditions," *IEEE Trans. Sustain. Energy*, vol. 9, no. 1, pp. 74–85, Jan. 2018.

[46] M. Alanazi, A. Fathy, D. Yousri, and H. Rezk, "Optimal reconfiguration of shaded PV based system using African vultures optimization approach," *Alexandria Eng. J.*, vol. 61, no. 12, pp. 12159–12185, Dec. 2022.

[47] D. Yousri, D. Allam, and M. B. Eteiba, "Optimal photovoltaic array reconfiguration for alleviating the partial shading influence based on a modified Harris hawks optimizer," *Energy Convers. Manage.*, vol. 206, Feb. 2020, Art. no. 112470.

[48] B. Aljafari, P. R. Satpathy, and S. B. Thanikanti, "Partial shading mitigation in PV arrays through dragonfly algorithm based dynamic reconfiguration," *Energy*, vol. 257, Oct. 2022, Art. no. 124795.

[49] A. Fathy, D. Yousri, T. S. Babu, H. Rezk, and H. S. Ramadan, "An enhanced reconfiguration approach for mitigating the shading effect on photovoltaic array using honey badger algorithm," *Sustain. Energy Technol. Assessments*, vol. 57, Jun. 2023, Art. no. 103179.

[50] E. R. Sanseverino, T. N. Ngoc, M. Cardinale, V. Li Vigni, D. Musso, P. Romano, and F. Viola, "Dynamic programming and Munkres algorithm for optimal photovoltaic arrays reconfiguration," *Sol. Energy*, vol. 122, pp. 347–358, Dec. 2015.

[51] D. Yousri, S. B. Thanikanti, K. Balasubramanian, A. Osama, and A. Fathy, "Multi-objective grey wolf optimizer for optimal design of switching matrix for shaded PV array dynamic reconfiguration," *IEEE Access*, vol. 8, pp. 159931–159946, 2020.

[52] M. N. R. Nazeri, M. F. N. Tajuddin, T. S. Babu, A. Azmi, M. Malvoni, and N. M. Kumar, "Firefly algorithm-based photovoltaic array reconfiguration for maximum power extraction during mismatch conditions," *Sustainability*, vol. 13, no. 6, p. 3206, 2021.

[53] P. R. Satpathy, R. Sharma, and S. Jena, "A shade dispersion interconnection scheme for partially shaded modules in a solar PV array network," *Energy*, vol. 139, pp. 350–365, Nov. 2017.

PRADYUMNA MALLICK received the B.Tech. degree in electrical engineering and the M.Tech. degree in power system engineering, in 2012 and 2015, respectively. He is currently pursuing the Ph.D. degree with Siksha 'O' Anusandhan Deemed to be University, Bhubaneswar, India. He is a part-time Research Scholar with Siksha 'O' Anusandhan Deemed to be University, Bhubaneswar. Also, he is an Assistant Professor with the Rajdhani Engineering College, Bhubaneswar. His research interests include solar PV systems, microgrids, and smart grids.

RENU SHARMA (Senior Member, IEEE) received the master's degree in electrical engineering from Jadavpur University, in 2006, and the Ph.D. degree in electrical engineering from Siksha 'O' Anusandhan Deemed to be University, Bhubaneswar, India, in 2014. She is currently a Professor and the Head of the Department of Electrical Engineering, Siksha 'O' Anusandhan Deemed to be University. She has published around 80 international journals and conference papers. She has around 20 years of leading impactful technical, professional, and educational experience. Her research interests include smart grids, soft computing, solar photovoltaic systems, power system scheduling, evolutionary algorithms, and wireless sensor networks. She is a Life Member of IE (India), a Member of IET, a Life Member of ISTE and ISSE, and the Chair of the WIE IEEE Bhubaneswar Sub Section. She was the General Chair of theIEEE ODICON 2021, flagship conference IEEE WIECON-ECE 2020, and Springer conference GTSCS-2020 and IEPCCT-2019. She is a Guest Editor of Special Issue on *International Journal of Power Electronics* and *International Journal of Innovative Computing and Applications* (Inderscience).

PRIYA RANJAN SATPATHY received the Ph.D. degree in solar photovoltaic power systems (electrical engineering) from Siksha 'O' Anusandhan Deemed to be University, India, under fellowship by CSIR, Government of India, in 2022. He is currently a Research Associate with the Department of Electrical and Electronics Engineering (EEE), Chaitanya Bharati Institute of Technology (CBIT), Hyderabad, India, under a project supported by Najran University, Saudi Arabia. He was a Senior Research Fellow with the Council of Scientific and Industrial Research (CSIR), from 2021 to 2022. He has reviewed more than 150 articles. His research interests include solar power systems, PV array efficiency improvement and fault reduction, maximum power point tracking, and PV system design and installation (off-grid and on-grid). He has depth knowledge of different PV system software, including PVSyst, PVSOL, Sketchup, Helioscope, and AutoCAD. He has published two Indian patents and more than 50 international journals and conferences. Also, he has been serving as an Associate Editor for Taylor and Francis and a Reviewer for many international conferences and journals, such as IEEE, Elsevier, IET, Wiley, Springer, Frontiers, Taylor and Francis, and Hindawi.

SUDHAKAR BABU THANIKANTI (Senior Member, IEEE) received the B.Tech. degree from Jawaharlal Nehru Technological University, Ananthapur, India, in 2009, the M.Tech. degree in power electronics and industrial drives from Anna University, Chennai, India, in 2011, and the Ph.D. degree from VIT University, Vellore, India, in 2017. He held a Postdoctoral Research Fellowship with the Department of Electrical Power Engineering, Institute of Power Engineering, University Tenaga Nasional (UNITEN), Malaysia. He was a Senior Research Associate with the Department of Electrical and Electronic Engineering Science, University of Johannesburg. Currently, he is an Associate Professor with the Department of Electrical and Electronics Engineering, Chaitanya Bharati Institute of Technology, Hyderabad. He has published more than 140 research articles in various renowned international journals. His research interests include the design and implementation of solar PV systems, renewable energy resources, power management for hybrid energy systems, storage systems, fuel cell technologies, electric vehicles, and smart grids. He has been acting as an Editorial Board Member and a Reviewer of various reputed journals, such as the IEEE, IEEE Access, IET, Elsevier, and Taylor and Francis.

NNAMDI I. NWULU (Senior Member, IEEE) is currently a Full Professor with the Department of Electrical and Electronic Engineering Science, University of Johannesburg, and the Director of the Centre for Cyber-Physical Food, Energy and Water Systems (CCP-FEWS). His research interests include the application of digital technologies, mathematical optimization techniques, and machine learning algorithms in food, energy, and water systems. He is a Professional Engineer registered with the Engineering Council of South Africa (ECSA), a Senior Member of the South African Institute of Electrical Engineers (SMSAIEE), and a Y-Rated Researcher by the National Research Foundation of South Africa. He is the Editor-in-Chief of the *Journal of Digital Food Energy and Water Systems* and an Associate Editor of *IET Renewable Power Generation* and *African Journal of Science, Technology, Innovation and Development*.